ISTANBUL TECHNICAL UNIVERSITY ★ GRADUATE SCHOOL OF SCIENCE ENGINEERING AND TECHNOLOGY

THE NUMERICAL EVALUATION OF JET IMPINGEMENT EFFECTIVENESS IN A BOTTOM OF CONFINED CAVITY

M.Sc. THESIS

Mehmet Fatih BAYAR

Department of Mechanical Engineering

Heat Transfer – Fluid Mechanics Programme

JUNE 2018

ISTANBUL TECHNICAL UNIVERSITY ★ GRADUATE SCHOOL OF SCIENCE ENGINEERING AND TECHNOLOGY

THE NUMERICAL EVALUATION OF JET IMPINGEMENT EFFECTIVENESS IN A BOTTOM OF CONFINED CAVITY

M.Sc. THESIS

Mehmet Fatih BAYAR

(503131116)

Department of Mechanical Engineering

Heat Transfer – Fluid Mechanics Programme

Thesis Advisor: Assistant Professor Dr. Murat ÇAKAN

JUNE 2018

İSTANBUL TEKNİK ÜNİVERSİTESİ ★ FEN BİLİMLERİ ENSTİTÜSÜ

DUVARLA SINIRLANDIRILMIŞ BİR KAVİTE TABANINDA JET ÇARPTIRMALI SOĞUTMA ETKENLİĞİNİN SAYISAL OLARAK İNCELENMESİ

YÜKSEK LİSANS TEZİ

Mehmet Fatih BAYAR

(503131116)

Makine Mühendisliği Anabilim Dalı

Isı-Akışkan Yüksek Lisans Programı

Tez Danışmanı: Yrd.Doç. Dr. Murat ÇAKAN

HAZİRAN 2018

Mehmet Fatih Bayar, a M.Sc. student of İTU Graduate School of Science Engineering and Technology student ID 503131116, successfully defended the thesis entitled "THE NUMERICAL EVALUATION OF JET IMPINGEMENT EFFECTIVENESS IN A BOTTOM OF CONFINED CAVITY" which he prepared after fulfilling the requirements specified in the associated legislations, before the jury whose signatures are below.

Thesis Advisor : **Assistant Professor Dr. Murat ÇAKAN** .....
İstanbul Technical University

Jury Members : **Associate Professor Dr. Emre ALPMAN** .....
Marmara University

Assistant Professor Dr. L. Ali KAVURMACIOĞLU .....
İstanbul Technical University

Date of Submission : 4 May 2018
Date of Defense : 4 June 2018

To my beloved family,

FOREWORD

Firstly, I would like to express my sincere thanks to Assistant Professor Dr. Murat ÇAKAN for his supervision, patience and helpful critics throughout this research project. I would also like to thank all instructors in the Department of Mechanical Engineering for their engineering insight to problems and for his valuable guidance throughout my study.

I acknowledge Ford Otosan for allowing me to pursue a graduate degree while working as a full time R&D Engineer.

My special thanks are due to my dear friends and colleagues who backed me up at difficult times to complete this study.

Finally, at last but not the least, I would like to thank Firdevs, Mehmet and Duygu BAYAR for each page of this academic research project. There is not the shadow of a doubt that, this study would not have completed if it were not for their endless support, encouragement and belief in me.

May 2018 Mehmet Fatih BAYAR

(Mechanical Engineer)

TABLE OF CONTENTS

Page

ABBREVIATIONS

CNC	**:** Computer Numerical Control
CFD	**:** Computational Fluid Dynamics
ANSYS	**:** Analysis System
RNG	**:** Re-Normalisation Group
SST	**:** The Shear Stress Transport
2D	**:** 2 Dimensional
3D	**:** 3 Dimensional
CPU	**:** Central Processing Unit

SYMBOLS

Re	**:** Reynolds Number
H	**:** Distance between circular jet and the bottom wall
D	**:** Diameter of jet nozzle
α	**:** Inclination of buttom surface
k-e	**:** Turbulent kinetic energy-epsilon
k-w	**:** Turbulent kinetic energy k-omega
K	**:** Kelvin
C	**:** Celcius
V	**:** Inlet velocity of jet nozzle
T	**:** Temperature of ideal gas
$\mathbf{T_a}$	**:** Reference temperature
S	**:** Sutherland temperature
μ_a	**:** Dynamic viscosity
y+	**:** Y plus
L	**:** Length of the jet nozzle
$\mathbf{U_\infty}$	**:** Inlet velocity of jet nozzle
$\boldsymbol{\nu}$	**:** Kinematic viscosity
$\mathbf{C_f}$	**:** Skin friction coefficient,
$\boldsymbol{\zeta_w}$	**:** Local wall shear stress
ρ	**:** Density
$\mathbf{y_p}$	**:** Minimum mesh length
P	**:** Total pressure
k	**:** Thermal conductivity
$\mathbf{C_\mu}$	**:** Experimental constant
$\mathbf{P_k}$	**:** Turbulent kinetic energy
$\bar{\mathbf{S}}$	**:** Average of strain rate sensor in terms of time
$\boldsymbol{\sigma_w}$, $\boldsymbol{\sigma_k}$	**:** Prandtl numbers in terms of k and w
t	**:** Time

LIST OF TABLES

Page

LIST OF FIGURES

Page

THE NUMERICAL EVALUATION OF JET IMPINGEMENT EFFECTIVENESS IN A CONFINED CAVITY

SUMMARY

There are many studies released about small air jet impingement in today's world and the number of studies and usage areas have been increasing in this direction day by day. Because the size of design of applications are becoming smaller due to ergonomic requirements.

There are widely small jet usage area available in the industry in connection with their mass and heat transfer capability and being package friendly. To mention about where they are used; they can be collected under three title. They are drying, cooling and heating. The most common area is the area which is using cooling ability of jet nozzle. In this direction, cooling ability can be divided into two topics as protection and production skill. For example, internal combustion engines, jet engines and some applications in heavy industry (CNC turning, milling etc.), electronic systems require efficient cooling systems to reach better performance and prevent hardware failure. These usage areas use protection skills of jet nozzle. To give an example, obtaining tempered glass method is populer in using production method of jet nozzle. Because, the procedure of production of tempered glass need quick cooling after it gets its melting temperature. The jet nozzle is used due to its heating ability as well. Some products are desired high temperature to stay healthy. However, the storage areas of the products may not have the necessities about temperature. For this reason, jet nozzle heating method is finding a solution to avoid it.

Associated with ever growing usage areas of jet nozzle, the design of jet nozzle is becoming important role to get higher effectiveness. The unconscious applications can cause cost and efficiency reduction. In this study, the best design schematic is being tried to find to prevent it.

This study is related to time dependance heat transfer characteristics of small jet impingement under variety condition of flow type, the distance between the jet and the bottom wall, the inclination of bottom wall and the blockage effect on the way of flow line on the bottom cavity (293°K). To mention in details with pointing out using air as refrigerant, the first factor is flow characteristic related different Reynolds number (Re) changes in two values of 3,300 to 6,600 which are affected directly from diameter, inlet velocity of circular jet nozzle and kinematic viscosity of air in this inlet temperature (283°K). The second one is to see effect of distance between circular jet and the bottom wall (H) and constant nozzle diameter with 10 mm (D) (H/D) as three different ratio of 1, 5, 10. The third one is the tilt angle of bottom wall which is nearly the first contact with the jet flow with variance of 0, 10 and 20 degrees. The last one is using circular blockage over flow area. Unstructured and structured mesh type are used by looking inclination availability. If the geometry has

zero inclination, structured and quadriteral mesh is used. Otherwise, unstructured and triangle mesh is applied at inclined zones. Standart wall function k-e turbulent model is performed all of the simulations. For the validation, standart wall function k-e, realizable k-e and SST k-w turbulent model are compared with one simulation. It is seen that the results are close to each other so it is not problem to continue with standart wall function k-e turbulent model. Lastly, the solution is run by using 2-D and transient method.

Totally there are about twenty configurations simulated in the study by changing inputs which have mentioned before. As a consequence of these tests, the first deduction is to impinge the air with as fast as possible to the taget surface since the heat transfer on the surface has directly relationship with Reynolds number namely inlet velocity. Another method of getting increased Reynolds number might be widen diameter of jet nozzle. It also causes efficient heat transfer. The second deduction is to pull the jet nozzle over the surface which is desired to cool, in another saying reduce the distance between the jet nozzle and the effected plate since the effect of air has improved in this case. The third inference is applying inclination has poor effect on the heat transfer between air exit from jet nozzle and the target plate due to nonuniform flow distribution. All these inputs lead quick cooling as well besides increased cooling profile. The last inference is setting blockage on the flow line can be used for increasing head transfer capability but it does not work for increasing cooling acceleration.

In conclusion, the lower distance between target plate and jet nozzle, the more Reynolds number, the less inclination and using blockage on the flow line is the best configuration to increase cooling and heat transfer capacity on the confined cavity.

DUVARLA SINIRLANDIRILMIŞ BİR KAVİTEDE JET ÇARPTIRMALI SOĞUTMA ETKENLİĞİNİN SAYISAL OLARAK İNCELENMESİ

ÖZET

Günümüz dünyasında küçük boyutlarda jetin çarptırmalı soğutma etkinliği üzerine birçok çalışma yapılmaktadır. Mevcudiyette olan çalışmaların yanında da bu konu üzerindeki gerek çalışma gerekse de kullanım alanı olarak yoğunlaşma günden güne artmaktadır. Bunun altında günümüzde kullanılan uygulamaların dizaynının ergonomi arttırımı kapsamında gittikçe küçüldüğü gerçeği yatmaktadır.

Giriş paragrafında da bahsedildiği üzere günümüz endüstrisinde küçük boyutlarda jet çarptırmalı soğutma uygulamasının yüksek kütle ve ısı transferi kapasitesi ve küçük uygulamalara yatkınlığından ötürü geniş bir kullanım alanı mevcuttur.

Bu alanların nereleri olduğundan bahsedecek olursak; kullanım alanları kurutma, soğutma ve ısıtma olmak üzere üç ana başlıkta toplanabilir. Bu alanlar içinden en yaygın olanı ise hiç kuşkusuz jet akışı soğutma kabiliyetinden ötürü kullanan alanlardır. Soğutma kabiliyeti de kullanım yerine göre kendi içinde koruma ve üretim alanları olarak ikiye ayrılmaktadır.

Örnek olarak, çok yüksek sıcaklıklarda çalışan içten yanmalı, jet motorları, ağır sanayideki bazı uygulamalar (torna,freze vs.), elektronik sistemler daha yüksek performanslara erişebilmek ve oluştuğu parçaların dayanım limitleri için etkili bir soğutma sistemine ihtiyaç duymaktadır. Bu uygulamalar jet soğutmanın koruma alanlarındandır.

Jet soğutmanın üretim teknolojilerinde kullanılma alanına dönersek, temperli cam, camın ergime sıcaklığına kadar ısıtılıp ani olarak soğutulması ile elde edilmektedir buradaki hızlı ve etkili soğutma, jetin soğutma kabiliyeti ile yapılmaktadır. Yani jet hızlı soğutmaya sebep olarak üretim tekniğinde bir adım olmaktadır. Jet akışın soğutma özelliğinin yanında birkaç alanda da ısıtma kabiliyetinden de yararlanılmaktadır.

Bir örnek olarak, bazı ürünlerin saklandıkları depolarda sağlıklı kalabilmesi için gerekli olan minimum sıcaklık limitinin altına düştükleri, bunun önüne geçmek için de çözüm önerisi olarak jet akışların belirlenen mimimum sıcaklıklarda devreye girerek ürünlerin sıcaklıklarını yükseltmesi gösterilebilir.

Jet soğutma uygulamalarının revaçta olduğu ile bağlantılı olarak, jetin hangi şartlar altında en iyi soğutmayı yapabileceği üzerine dizayn çalışmaları da önem kazanmıştır. Bilinçsiz şekilde yapılan dizaynlar ve uygulamalar hem ücret hem de verim kaybına yol açmaktadır. Bu gibi durumları önlemek için bu çalışmada en iyi jet soğutma koşullarını ve dizayn şemasını anlatılmıştır.

Bu çalışmada küçük boyutlardaki jetin çarptırmalı soğutma uygulamasının hedef plaka üzerindeki zamana bağlı ısı transfer karakteristiği incelenmektedir. Çalışmada hava soğutması kullanılmış olup havanın jete giriş sıcaklığı sabit 283°K alınmıştır.

Bunun yanında soğutmanın istendiği hedef plakanın sıcaklığı da başlangıç koşulu olarak 293°K kabul edilmiştir.

Isı transfer karakteristiği saptanması kapsamında akış türü, jet ile hedef tabaka arası uzaklık, hedef tabakanın eğimi ve akış jetten çıkış yaptıktan sonraki doğrultusuna engel konulması olarak dört başlık altında çalışmalar yapılmıştır.

Bu başlıkların detayına inersek, incelenen ilk faktör 3,3300 ve 6,660 olarak hesaplanan Reynolds sayısı ile elde ettiğimiz akış karakteristiği etkisidir. Bilindiği gibi Reynolds sayısı akışkanın jete giriş hızı, akışkanın girdiği kesitin çap değeri ve akışkanın giriş sıcaklığındaki kinematik akmazlık değeri ile doğrudan ilgilidir.

Bu çalışmada Reynolds sayısının değeri enjektöre giren havanın sabit sıcaklık ve çap değeri olduğundan ötürü havanın giriş hızının değişmesi (5-10 m/s) ile farklılık göstermektedir.

İkinci faktör, dairesel jet ile hedef plaka arasındaki uzaklığın (H), havanın girdiği enjektör çapına (D) oranı (H/D) yani dolaylı olarak jet ile hedef plaka arasındaki uzaklık etkisidir. Sabit enjektör çapında (10 mm), jetin plakaya uzaklığı değiştirilerek (10,50,100 mm) üç farklı oran (1,5,10) incelenmiştir.

Üçüncü faktör olarak soğutulmasını istediğimiz hedef plakanın eğiminin (0°,10°,20°) soğutma profiline etkisi gözlenmiştir.

Son olarak incelenen konu ise akış üzerine yerleştirilen bir engelin hedef plaka soğutma profili üzerine etkisi olmuştur.

Çalışmada kullanılan mesh tiplerine değinirsek, yapısal ve yapısal olmayan olmak üzere iki farklı mesh türü kullanılmıştır. Eğim olmayan geometrilerde düzenli olduğundan ötürü yapısal ve kare mesh kullanılırken eğimli geometrilerde düzensiz olan eğimli kısımlar yapısal olmayan ve üçgen mesh uygulamasına tabii tutulmuştur. Uygun mesh sonrası tüm simulasyonlarda standart duvar fonksiyonu k-e türbülans modeli kullanılmıştır.

Uygun modelin kullanılıp kullanılmadığı doğrulaması için standart duvar fonksiyonu k-e, gerçeklenir k-e, kayma gerilmesi k-w türbülans modelleri ile bir uygulamada karşılaştırma yapılmış ve çıkan sonuçlar arasında küçük farkların olduğu görülmüştür. Bundan dolayı standart duvar fonksiyonu ile çözüme devam edilmiştir. Ayrıca tüm simulasyonlar iki boyutlu ve zamana bağlı olarak çözülmüştür.

Çözüm için gerekli koşullar sağlandıktan sonra bahsettiğimiz etkenler değiştirilerek toplamda yirmi civarında dizayn konfigurasyonu koşulmuştur. Bu testlerin sonucuna göre bazı çıkarımlar edinilmiştir.

İlk çıkarım, Reynolds sayısının artması, hedef plaka soğuma profili üzerinde olumlu etki göstermiştir. Bu sebepten yola çıkarak daha soğuk bir tabaka için Reynolds sayısını arttıracak bütün aksiyonlar yani jet enjektörüne giren havanın hızının ve havanın girdiği enjektör çapının arttırılması örnek olarak uygulanmalıdır. Reynolds sayısı ile ısı geçişi kapasitesi doğru orantılı olduğundan bu sonuç olağandır.

İkinci çıkarım, jetin soğutulması istenen hedef plakaya yaklaştırılması diğer bir deyişle jet ile hedef plaka arasındaki mesafenin azalması hedef plakanın daha soğuk sıcaklıklara gelmesine sebep olmuştur. Bundan ve akışın çarpan etkisinin fazla olmasından dolayı jetin hedef tabakaya olabildiğince yakınlaştırılması soğutma verimini yukarıya çıkaracaktır.

Üçüncü çıkarım ise jetin soğutma etki performansının eğimli yüzeylerde daha zayıf olduğudur. Bunun nedeni, akışın düzgün dağılmamasından dolayı jet çıkışındaki hava ile hedef plaka arasındaki ısı transferinin kötü olmasıdır.

Bu doğrultuda ek olarak eğimli yüzeylerdeki eğime bağlı basınç ve sıcaklık dağılımı da ayrıca incelenmiştir. Bahsettiğimiz soğutma profilini iyileştiren üç etken aynı zamanda hızlı soğuma zamanlaması performanlarını da daha iyi noktalara getirmektedir.

Son etki olarak incelenen akış yönüne engel konulması da soğutma profiline olumlu katkı yapmıştır. Bu katkının aksine yöntemin, soğutma zamanlaması olarak engel akışın doğrudan etkisine kötü yönde etki ettiği için uygun olmadığı görüşmüştür.

Sonuç olarak, jet ile hedef plaka arasındaki mesafenin olabildiğince kısaltılması yani jetin hedef plakaya yakın etki ettirilmesi, akışın Reynolds sayısını arttırıcı aksiyonlar alınması, soğutulacak hedef plakanın eğimli olmaması ve akış yönüne konulacak engel soğutma konfigurasyonu olarak en uygun seçim olarak belirlenmiştir.

Yapılacak dizaynların ve ortam şartlarının bu doğrultuda seçilmesi hem maliyet hem de verime olumlu katkıda bulunacaktır.

1. INTRODUCTION

There are commonly usage areas available and used for small jet jets due to their much higher local mass and heat exchange coefficients in many industries. For the sake of example, the applications can be sorted in three main topics. Drying, cooling and heating are most common using area of jet impingement heat transfer. Small jet flows are employed in a widely areas for example surface area cleaning, cooling procedure of electronic devices due to meet the required performance, shaping and cutting of metal parts, cooling and lubricating of having high speed turbine and compressor blades and surface of combustion chamber, diesel engine cylinder head and base angine cooling , drying of textiles, cooling of fast food industry, paper cooling etc.

First of all, such as the forming of metal industry and nuclear plants which need at least 800-1000°C temperature for starting process, cooling of hot surfaces has vital requirement to continue the process without failure. Generally jet impingement cooling is preferred as it is easy to apply and classical [5]. In order to increase the turbine efficiency and power, operating higher temperature is required for modern gas turbine systems to better performance but in one hand while turbine desires higher temperature, it can be destructive by exceeding the material hardware temperature limit for the turbine parts such as blades, miles etc. Therefore, to get better performance through heat operation in the chamber, usage of improved cooling technologies is essential. Jet impingement cooling is one of the best effective techniques around improved cooling technologies [8].

The other application used small jet is glass tempering process. In these area, to provide more strength the ultra thin glass must be tempered. In the course of the tempering process, heating the glass until its melting temperature is first procedure and then applied quenching process which means very high pressure cooling to provide strength named tempered glass by using cooling time differences between inner and outer surface of glass. Quick cooling provides faster cooling performance for the outer surface of the glass than the center. As the center of the glass cools, it

tries to pull back from the outer surfaces. As a result, the center remains in tension, and the outer surfaces go into compression, which gives tempered glass its strength. Jet impingement is used for sudden cooling of thin glass which needs shorter cooling time and faster surface cooling during the glass tempering [3].

One of the usage areas for jet impingement is food engineering process. Food engineering process means analysing of procedures, quality conditions and process of producing plant level. The most serious investigation area of food engineering is treatment of lower temperature during pre-storage in the protected areas. To prevent low temperature problem, jet impingement cooling by air can be seen traditional cooling method even if lower Reynolds which is close to transient side [2].

As seen above mentioned studies, there are different widely usage areas available for the jet cooling impingement system. Impinging jets are well recognised as most efficient way to make easier process.

The purpose of this study is to investigate the effects of factors which influence cooling performance of jet impingement system in four main topics to specify the best and efficient approach. The flow type which is obtained from different inlet velocity of jet, the distance between the bottom surface wall and jet flow outlet, bottom surface inclination and obstacle on the way of jet flow. Transient effect of jet implecement, it is useful to examine the transient heat transfer characteristics of air impinging jets under conditions of between small jet plate distances and low temperature differences between the inlet and plate.

The inspected study is conducted with different Reynolds number (Re) changes from 3,000 to 6,000 which is connected with different inlet velocity of small jet 5 and 10 m/s in constant 10 mm circular diameter of small jet. The flows are accepted in turbulent class in reference to the Reynold numbers and taken an action accordingly. The ratio of the distance between outlet of circular jet and the bottom wall (H) and nozzle diameter with 10 mm (D) (H/D) differs in three class as 1 & 5 &10.

Bottom surface inclination which is thought having an important role for the cooling consist of no slope & 10° & 20°. Apart from these, circular blockage effect on the flow line is investigated. In additon to that, the meaning of the symbols used for the study are seen as below Table 1.1.

Table 1.1 : The most using symbols in the study [18].

Symbols	Descriptions
D	Nozzle diameter (mm)
H	distance between outlet of circular jet and the bottom wall (mm)
V	inlet velocity (m/s)
α	inclination of bottom wall (°)

2. LITERATURE SURVEY

Small jet impingement flow supply one of the most influential ways to interchange heating energy with convection between the wall and air while air phase condition is steady and the same. Therefore, small jet impingement is still demanded and has widely use at industrial applications. As a result of this demand, small jet impingement is getting more and more attractive topic from academic world. In other words, there are many studies available about small jet impingement usage areas existingly and is still worked on it. In this chapter, some studies about jet impingement will be examined from the point of usage areas & methods & methodology.

The first usage area mentioned this chapter is at industrial glass tempering unit. In these area, to provide more strength the ultra thin glass must be tempered. In the course of the tempering process, heating the glass until its melting temperature is first procedure and then applied quenching process which means very high pressure cooling to provide strength named tempered glass by using cooling time differences between inner and outer surface of glass [3]. Quick cooling provides faster cooling performance for the outer surface of the glass than the center. As the center of the glass cools, it tries to pull back from the outer surfaces. As a result, the center remains in tension, and the outer surfaces go into compression, which gives tempered glass its strength. Jet impingement is used for sudden cooling of thin glass which needs shorter cooling time and faster surface cooling during the glass tempering [10].

In the study of heat transfer and flow characteristics of the cooling system of an industrial glass tempering unit, the aim of the this paper is to simulate the heating process of the glass from beginning to tempered phase in reference to current industrial applications. As difficulty of the prepare set up and replicate the heating & cooling process like real word, computational fluid dynamics (CFD) is applied for the study. The results taken by ANSYS are compared with experimental data studied. Experimental scheme of the study (Figure 2.1) have nozzle rows which are on the production of glass area and interconnected with air compressed hoses that supply

5000 & 20000 m³/h air flow and 10 & 60 hPa. Glass forming is main factor to decide how many nozzle raws should be aligned.

The nozzles have 225 mm height, 1422 mm length, 100 mm width as it can be seen in Figure 2.2 and connected to compression chamber with 140 mm diameter hoses. The air from nozzles passes directly a 55 of 5.5 mm diameter & 18 mm pitch holes. The distance between rows is 25 mm. There is 50 mm distance between the nozzle and the square glass and the ratio of this distance and nozzle diameter is H/D = 9.1. The system of cooling can be seen from Figure 2.3. [10]

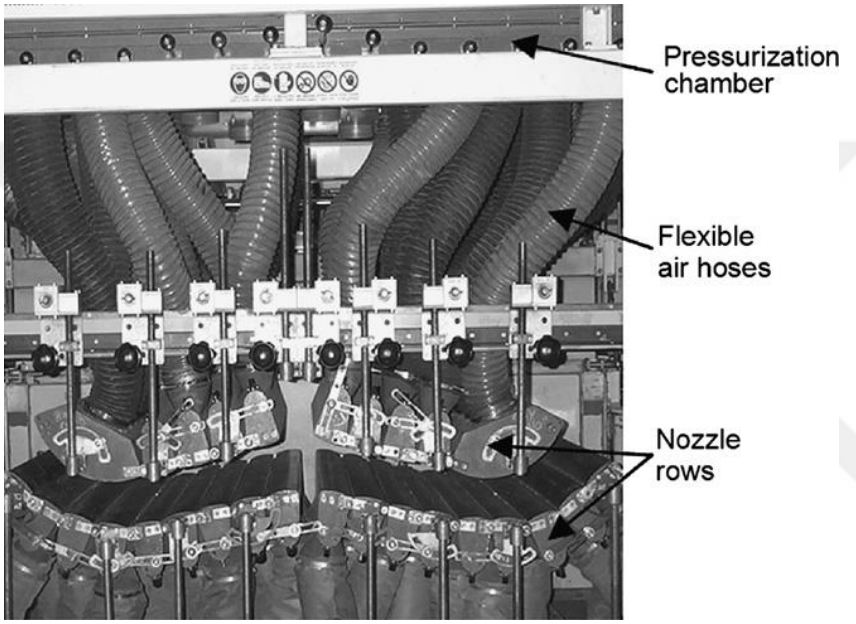

Figure 2.1 : Experimental scheme of the study of tempered glass cooling [10].

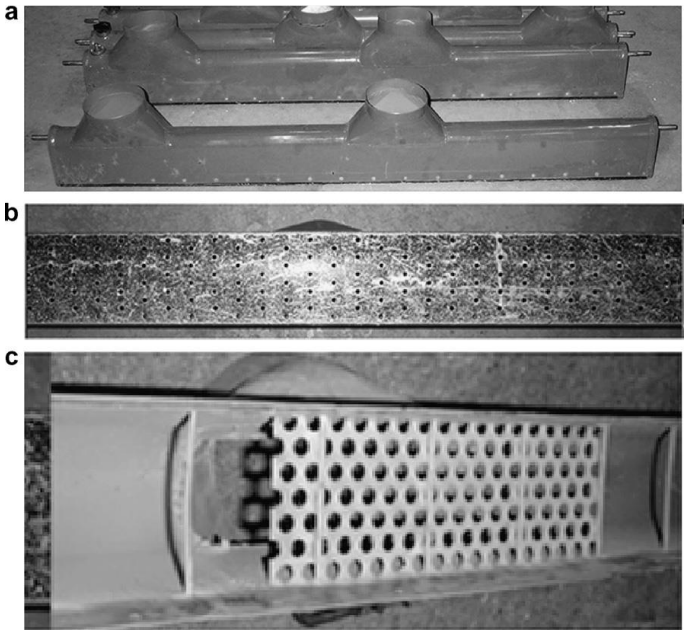

Figure 2.2 : The jet nozzles [10].

Figure 2.3 : The cooling system of tempered glass [10].

In numerical method, the six nozzles are accepted the same and the effect of gravity is neglected. The glass is also homogeneous. The flow consists of two regions as uniformity and tempering zone.

The Navier–Stokes equations with Reynolds averaged are calculated with second-order upwind solution for central differencing for diffusion finite element method. Sutherland's law is also used as below 2.1.

$$\mu(\mathrm{T}) = \mu_a \left(\frac{T}{T_a}\right)^{1/2} \frac{T_a + S}{T + S} \tag{2.1}$$

$$S = 110\ \mathrm{K}$$

$$T_a = 298\ \mathrm{K}$$

$$\mu_a = 1.85 \times 10^{-5}\ kg/ms$$

For H/D = 2, the RNG and standard k-e model is very close to experimantal data while for H/D=6, the results show that RNG k-e model is much more applicable so it is used for all calculations as the ratio is 9.1. The comparison can be seen from below figure 2.4.

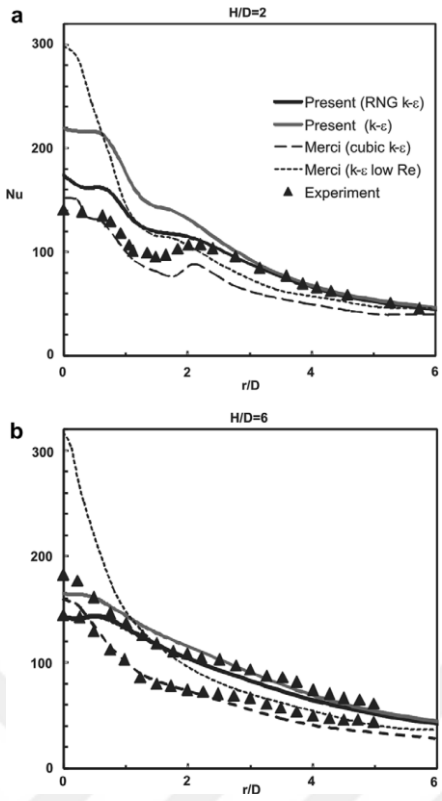

Figure 2.4 : Turbulent model comparison for different H/D ratio [10].

The nozzle grid is totally unstructured and there are about about 3,150,000 tetrahedral cells numerical grid. As shown in Figure 2.5, grid density is used much more than the other locations.

The other mesh surface discretisation is essential to understand that the tetrahedral cells are within the $50 < y+ < 150$.

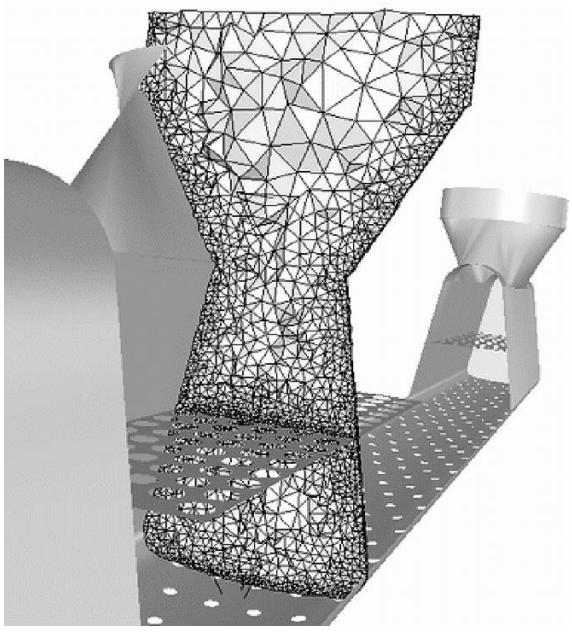

Figure 2.5 : Nozzle mesh distribution [10].

The cooling flow field is both structured and unstructured domain as glass plate is not complicated and around jet holes and nozzles, the regions are getting more complex. There are about about 1,500,000 tetrahedral cells numerical grid with 0.1 to 30.1 mm³ as shown in Figure 2.6, grid density is used much more than the other locations. The other mesh surface discretisation is essential to understand that the tetrahedral cells are within the 5< y+ < 41.

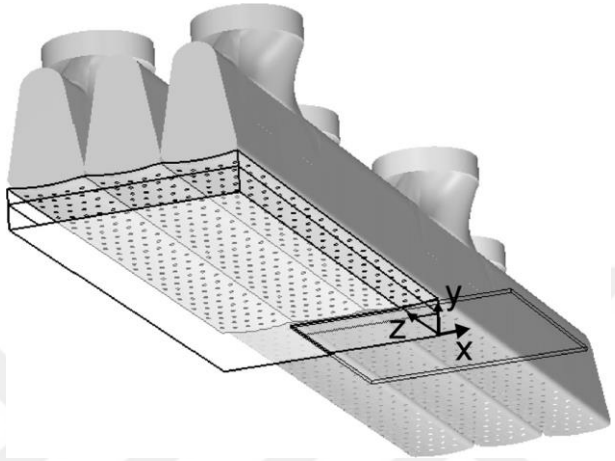

Figure 2.6 : Grid density [10].

As a result of selection of mesh type and turbulent model, the results are obtained. The transient temperature is solved about 90 s and it is compared with pyrometer measurement near nozzle set. The range of coeffients of heat transfer is between 150 and 250 W/ m² K. The results show that the least deviation between calculated and measured data is at 210 W/ m² K. At this point, the maximum relative error is about 4% while average on is 2% as Figure 2.7.

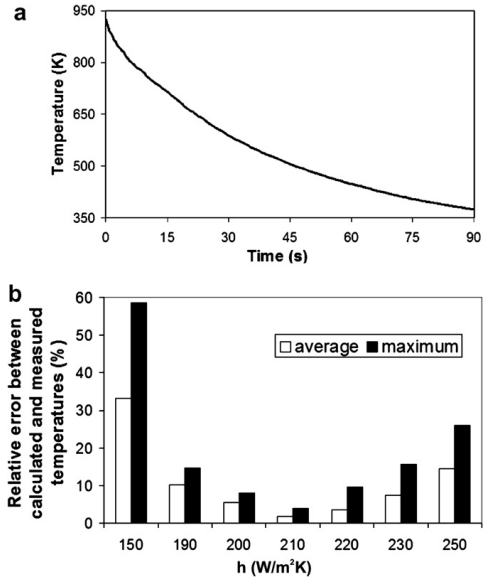

Figure 2.7 : Relative error comparison in terms of time [10].

This study provides a deep insight in the nozzles design and tempering zone importance for improvement of air flow to get better heat transfer to glass surface [3].

Another study about tempered process is transient heat transfer characteristics of small jet impingement on high-temperature flat plate [18]. The aim of this study is examinate the characteristics of heat transfer of small jet impingement when the distance between plate and jet is small and the difference between them is higher. The geometry consists of two components; circular tube and glass plate as seen Figure 2.8. The air passes from circular tube which is thought that has better heat transfer efficiency with 5 mm diameter and 6 mm height. The air strike directly to glass plate with 50 mm length & width and 2 mm thickness. The initial temperature of glass plate is 953 K while air is 298 K. and the flow is accepted three dimensionel, turbulent and incompressible and radiation effect is neglected. All walls are assumed adiabatic and air outlet boundary is determined pressure outlet like ambient pressure.

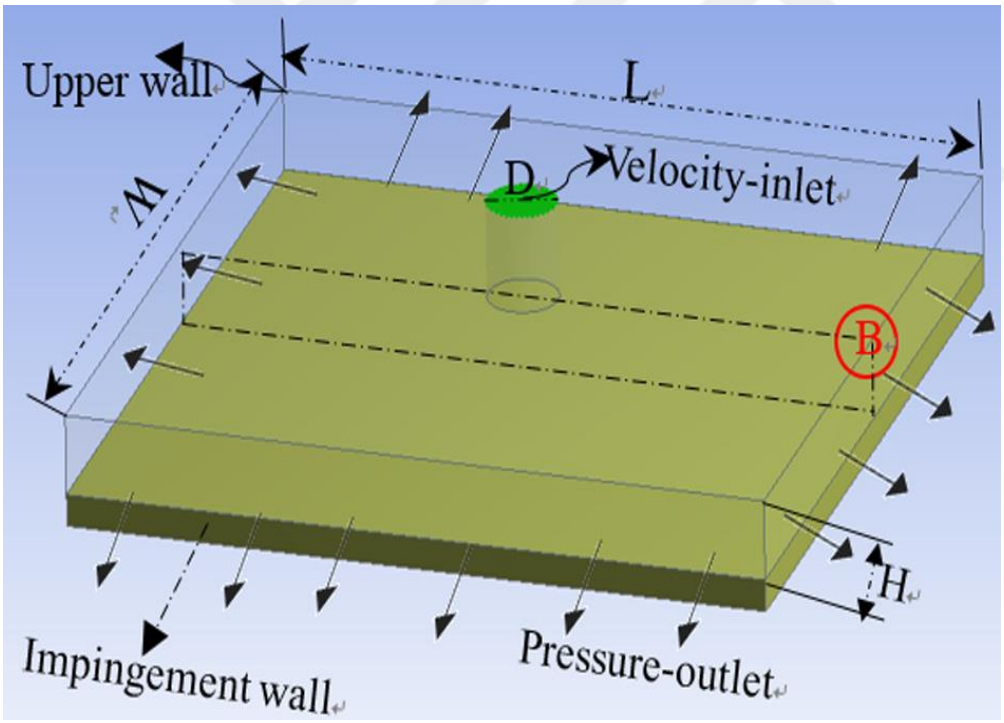

Figure 2.8 : The geometry of study [18].

The structural mesh is applied to get better grid quality near wall and target plate which the temperature gradients and flow are higher than others in. In addition to this, exemplary grid is also used where the distance with the jet and plate is 2 mm and as a result of grid independence analysis, 478,950 grid numbers of node is used in the following simulations as the reference of Figure 2.9.

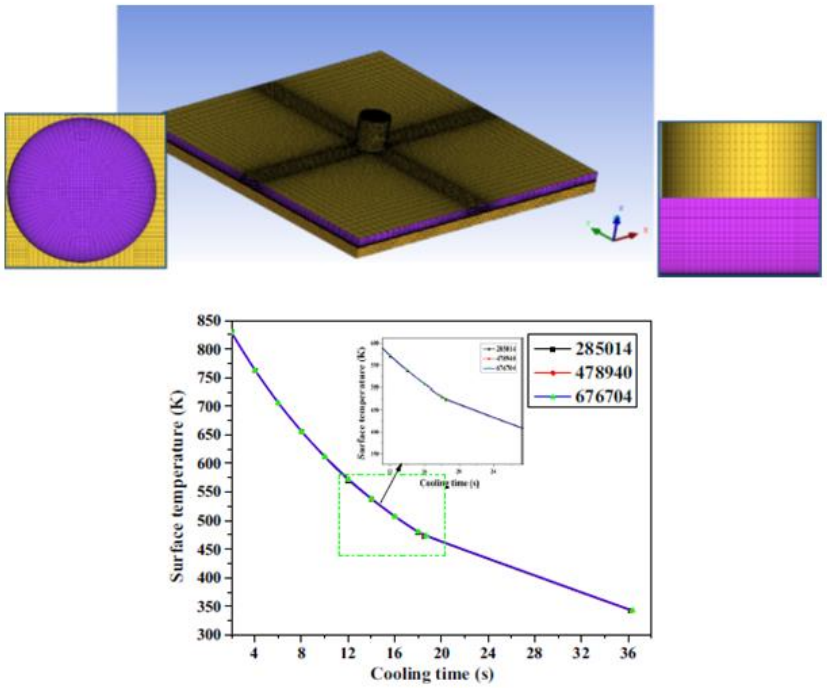

Figure 2.9 : The mesh plate and grid independence [18].

For turbulent model selection, the model with 30,000 Re, 8 mm diameter and 1 mm distance between flat and nozzle is selected.

In the study the experimental data is compared with turbulent models during 45 s cooling time of surface temperature in Figure 2.10. As a result of data, SST k-w turbulence model is accepted for the simulations as it simulates better than the others as a reference of experimentel data.

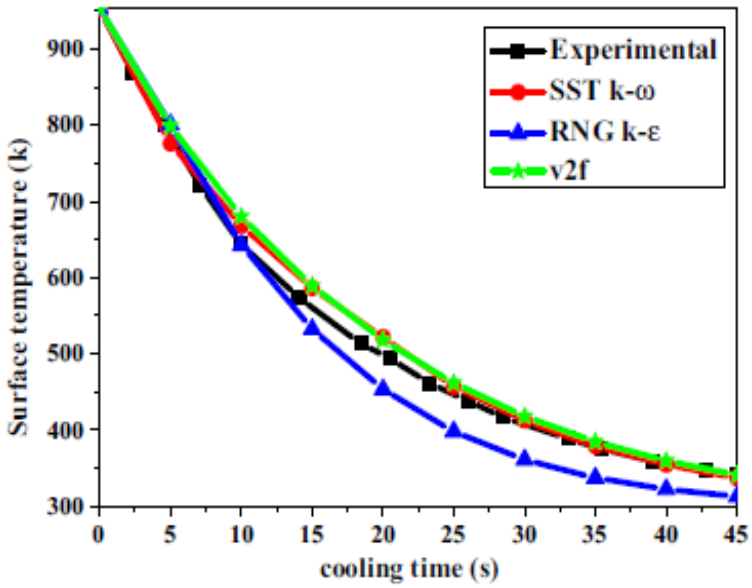

Figure 2.10 : Turbulent model comparison [18].

As a result of selection of mesh type and turbulent model, the results are obtained again[13]. The flat temperature is allowed to quench until 473 K. As shown from Figure 2.11 quenching time is decreased when the inlet velocity in other words reynolds number is increased under constant H/D values.

The other inference from Figure 2.11 is the quenching time with small H/D ratio is more than the bigger H/D set up. Furthermore, quenching times according to different H/D is less when the Reynolds is increased.

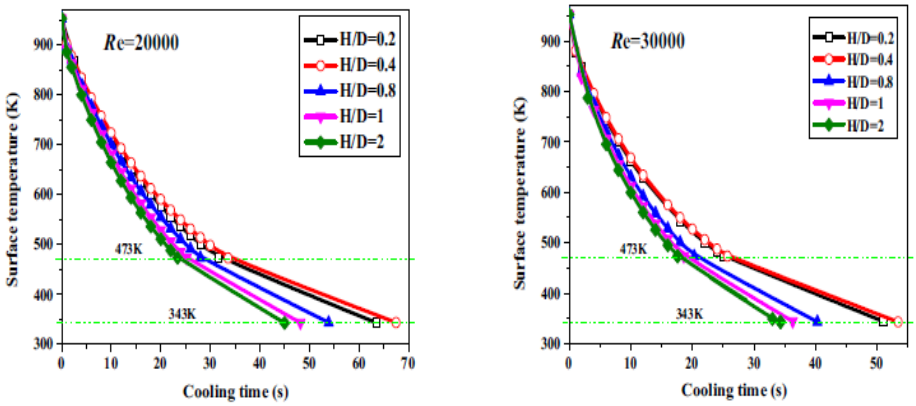

Figure 2.11 : Cooling time differences in terms of Re [18].

The other important result is temperature distribution form as it is significant to get better tempering glass. The temperature should be uniform to meet better tempered glass. From the point of Figure 2.12. It is seen that ΔT which is difference between stagnation and boundary point is increased first and after that decreased to quenching point. ΔT differs when H/D≤1 from H/D≥1. When the value of H/D increased, the temperature gradient is getting smaller. The heat transfer under transient case increases while Reynolds number is getting bigger.

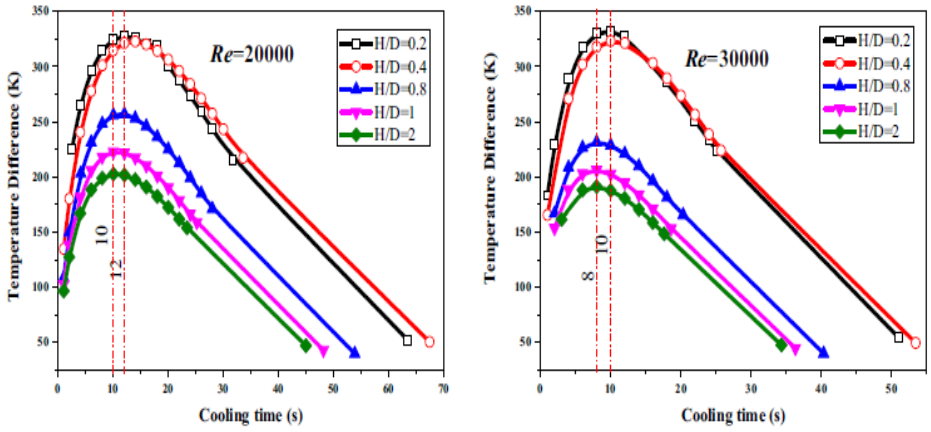

Figure 2.12 : Comparison of temperature gradient in terms of Re [18].

One of the study about jet impingement is food engineering process [2]. Food engineering process means analysing of procedures, quality conditions and process of producing plant level. The most serious investigation area of food engineering is treatment of lower temperature during pre-storage in the protected areas. To prevent low temperature problem, jet impingement cooling by air can be seen traditional cooling method even if lower Reynolds which is close to transient side. In this study, effective cooling heat transfer problems are examined in the industrial area. The turbulent flow with 23,000 Re is applied from 30 mm nozzle to 12 cm distance. The flow is incompressible and two dimensional. The impinged part has 3.5 cm diameter as Figure 2.13.

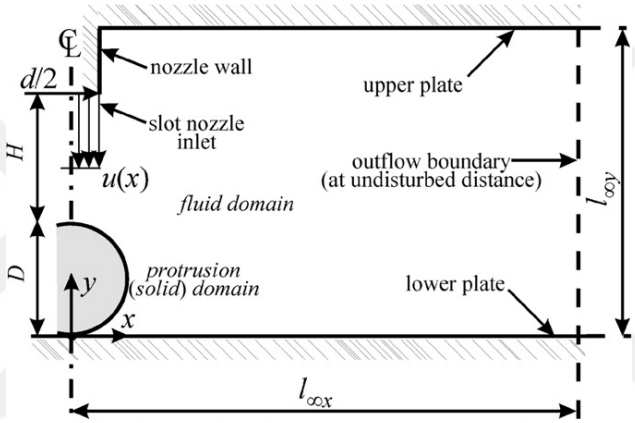

Figure 2.13 : The geometry of the study [2].

To allow better solution about pressure, temperature and velocity near the boundary layer, unstructured mesh with triangular pave grid is applied nearly 20,000 cells to the surface as seen Figure 2.14 and k-w Shear Stress turbulent model is used for the analysis.

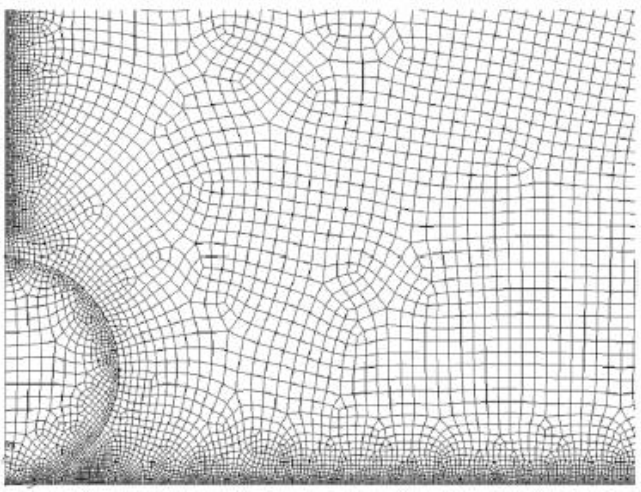

Figure 2.14 : Mesh distribution of the geometry [2].

In this study, localized force effect created by small jet impingement is reported and the heat flux non-uniform condition around the cylindrical surface is shown. The other result is when the food temperetaure initially equals with environment, cooling zone lie on its upper side. The flux distribution is as Figure 2.15.

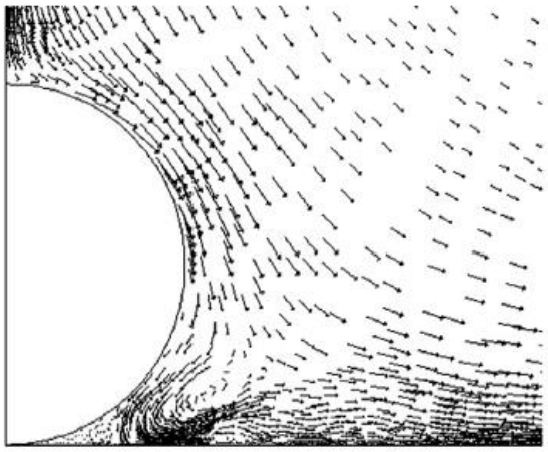

Figure 2.15 : Heat flux condition around the solid [2].

3. NUMERICAL METHODS AND METHODOLOGY

3.1 Numerical Set Up

3.1.1 Geometry

The geometry of the scheme is shown in Figure 3.1. In the study , the colder jet flow which is 283 degree Kelvin compared to 293 degree Kelvin bottom temperature impinging on the bottom surface which has the length of 400 mm by a circular jet. In other words, the inlet temperature of air in the jet is fixed at 10 degree Celcius, while the initial temperature of the bottom is 20 degree celcius.

In addition the jet flow is accepted to be two-dimensional, incompressible low turbulent flow which is almost in transition side. The jet shape is choosen circular due to get better heat transfer efficiency which has the constant 10 mm diameter and 200 mm height.

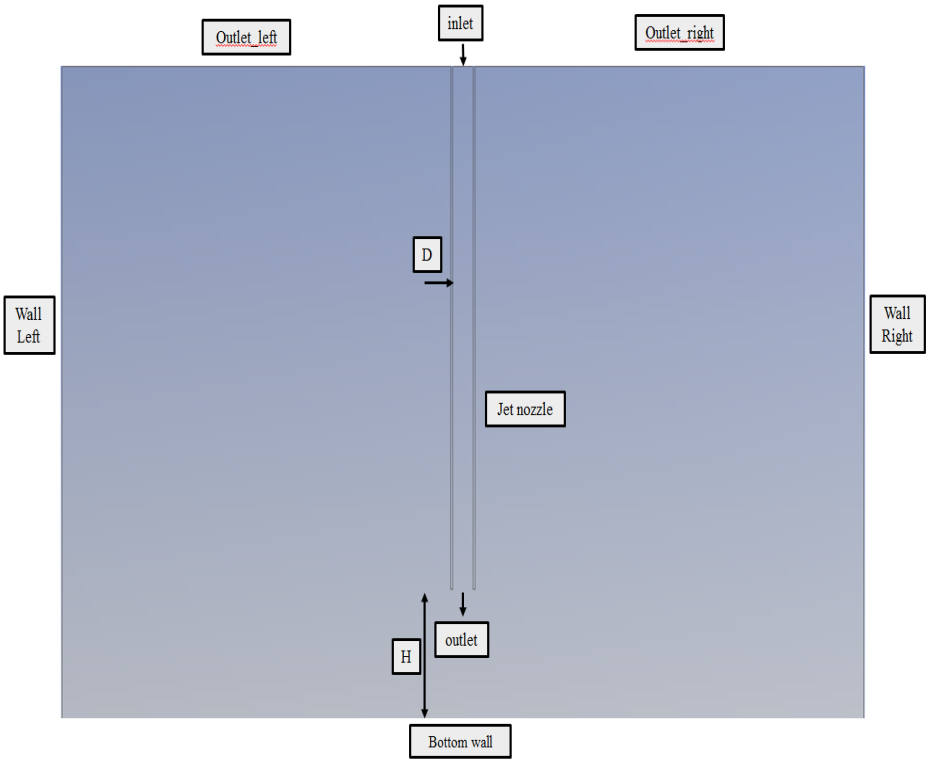

Figure 3.1 : Basic geometry of the study.

The two changeble factors in terms of geometry are distance between bottom surface and lower side of circular jet and the bottom surface inclination as seen Figure 3.2.

The effect of distance on the cooling performance is considered with 10 mm, 50 mm, 100 mm while bottom inclination vary from 0 to 20 degree.

All of the values used for the study can be seen below Table 3.1 and Table 3.2. In addition to that, our study is primary focused with the convective heat transfer of air jet impinging, also shown that the conduction and radiation effect is almost little on heat transfer.

In view of little effect on heat transfer, the effects of conduction and radiation heat transfer are ignored in our studies.

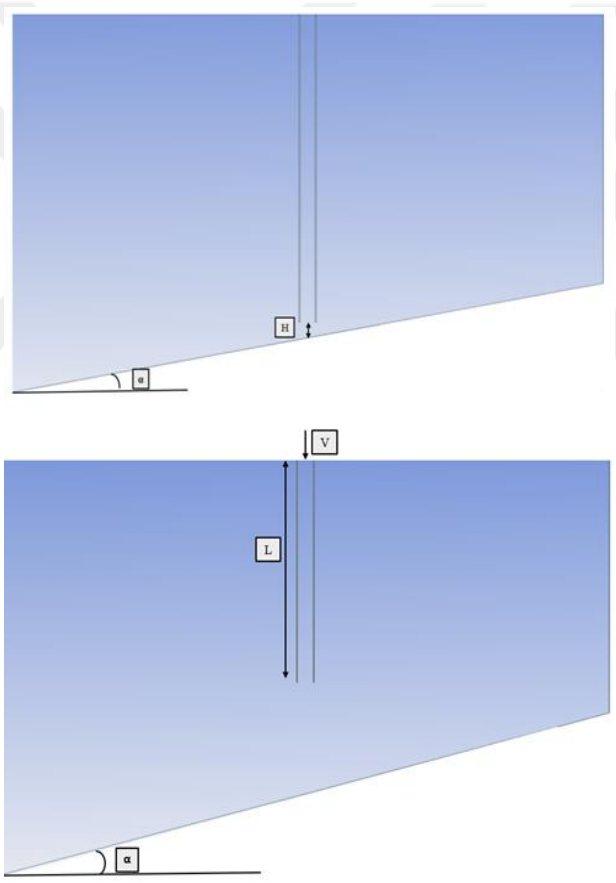

Figure 3.2 : Two of the configurations.

Table 3.1 : The inputs of the configurations.

V (m/s)	D (mm)	H (mm)	L (mm)	α (degree)
5 & 10	10	10 & 50 & 100	200	0 & 10 & 20

Table 3.2 : The configurations in terms of H/D and alpha.

H/D (mm/mm)	Alpha (degree)		
	0	10	20
1	Done	Done	Done
5	Done	Done	Done
10	Done	Done	Done

Apart from velocity, distance between bottom and jet and inclination effect on the tempereture distribution & average at the bottom, the obstacle impact is also investigated with one analysis as Figure 3.3 shows.

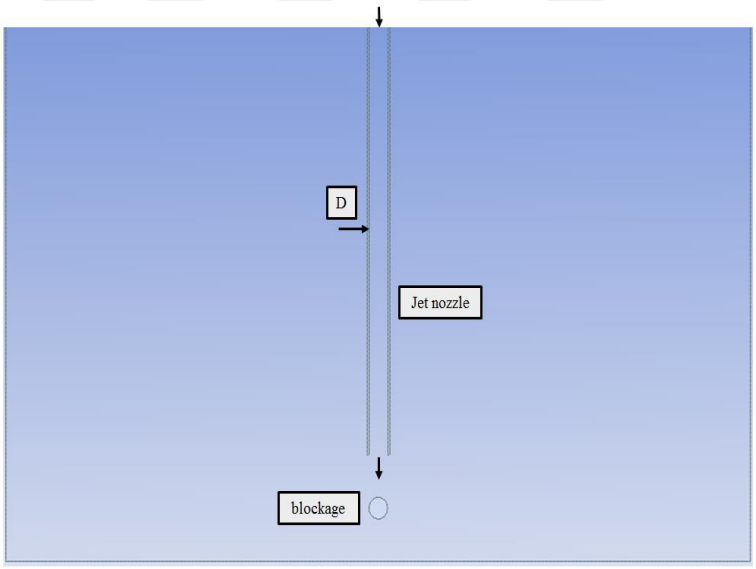

Figure 3.3 : The basic geometry of the study with blockage.

3.1.2 Boundary conditions

Jet nozzle: Jet nozzle is defined as a velocity inlet, the incompressible air flows under steady state and uniform condition with various Re numbers ($Re=U_{\infty}.D/\nu$). The inlet velocity of jet nozzle is 5 and 10 m/s so the Reynolds Numbers are 3300 and 6600 respectively. Another boundary condition about jet nozzle is inlet temperature which is 283 K.

Bottom, Right & Left Wall : The walls which are in the flow area are both adiabatic and has no slip.

Jet flow outlet: Air jet outlet is defined as a pressure outlet. The environment pressure is taken as references for the pressure of the air outlet.

Target plate: The target plate is defined as bottom wall. The bottom wall is adiabatic and has no slip.

Initial condition: At the beginning of the condition (t=0), the initial temperature of bottom and the other walls are 293 K except air inlet temperature. While time is ongoing, the jet nozzle is impinged, the temperatures of walls are decreased.

3.2 Methodology

3.2.1 Mesh type

What is meshing in simple words is, meshing divides to solid object into finite number of points which are interconnected with each other, and perform a complete solid. Therefore when someone run an analysis, software in the program apply equations on one point and get solutions. After that consider these results as a initial conditions to solve equations of next point. This process continue like this method until get results from the last points. There have been many mesh types created in reference to condition (shape, area etc.) of mesh object. Some common mesh types which are also used for this study are introduced in the following section. Basic example of the 2-D mesh is as Figure 3.4 [19].

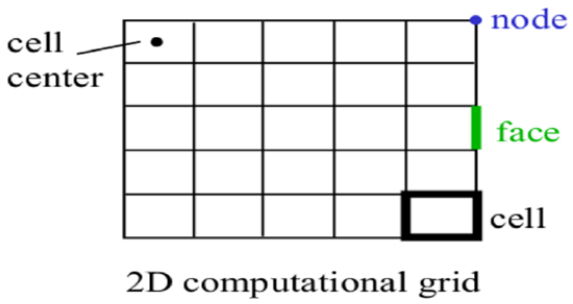

Figure 3.4 : Two dimension grid model [19].

3.2.1.1 Structured grids

Structured grids are defined by regular connectivity. The possible mesh element selections are hexahedral in 3D and quadrilateral in 2D in a computational rectangular selection.

In this study, quadrilateral mesh type is selected as the study is 2D. The model is high degree of space efficient since the next point relationships are identified by storage arrangement. It is represented with i, j, k indices. The advantages of structured mesh method are its comfortably use code, multi mesh and simplicity, better convergence and higher resolution over the unstructured mesh. Disadvantages of this mesh type are difficulty of create grids at multi block shapes and long time necessity for lasting grid domains for complex shape [19].

Quadrilateral: This mesh cell shape is a mainly 4 sided in one solid as it can be seen in the Figure 3.5. It is the most common cell shape in structured grids.

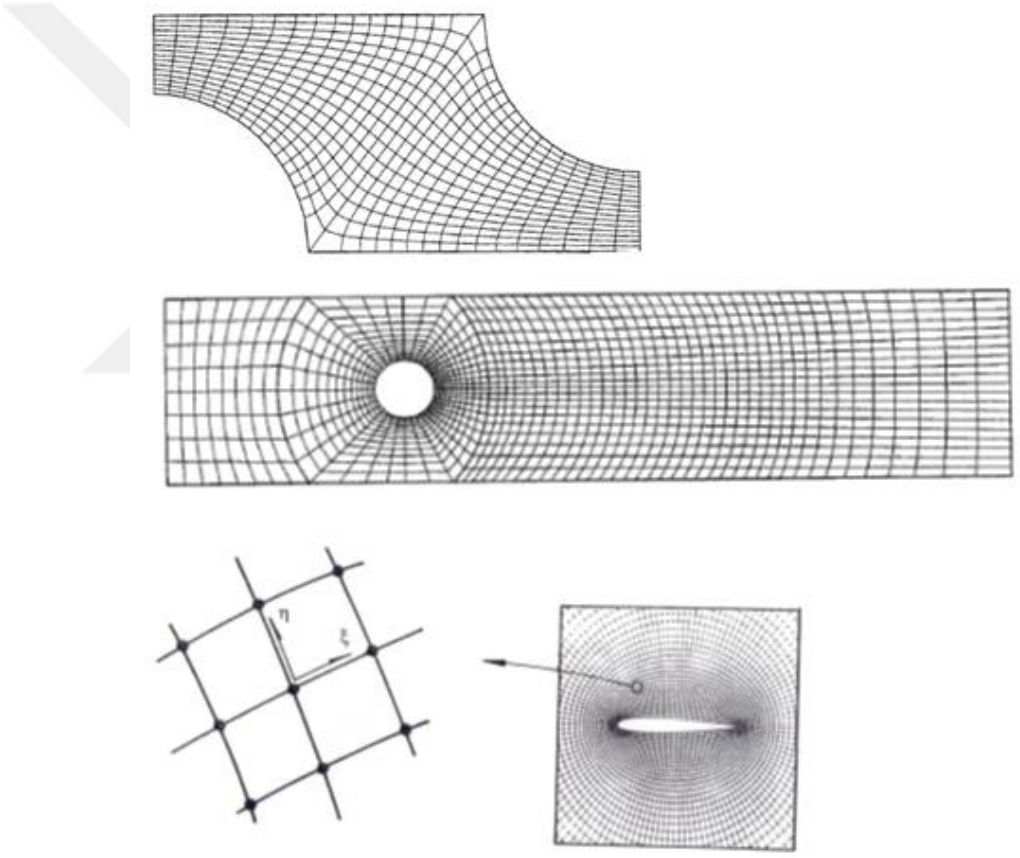

Figure 3.5 : Quadrilateral mesh cell shape [19].

3.2.1.2 Unstructured grids

An unstructured grid is defined by irregular connectivity. This grid cannot easily be mentioned as a two-dimensional or three-dimensional array in computational memory. This allows for any possible element to use and solve. When it is compared to structured meshes, unstructured model can be high degree space inefficient since

the next point relationships are identified by explicite storage arrangement. These grids are typically applied tetrahedra in 3D and triangles in 2D. It is represented with node numbers. The advantages of unstructured mesh method are not required long user time effort, lay out block structure and being very programmed type. It is also suitable for inexperienced users as it needs small inputs. Disadvantages of this mesh type are difficulty to find alternarive solutions and larger CPU&memory demand in the computer [19].

Triangle: This cell shape is mainly 3 sided in one solid as it can be seen in the Figure 3.6. It is one of the basic types of meshes. It is always quick and easy to generate. It is the most common cell shape in unstructured grids.

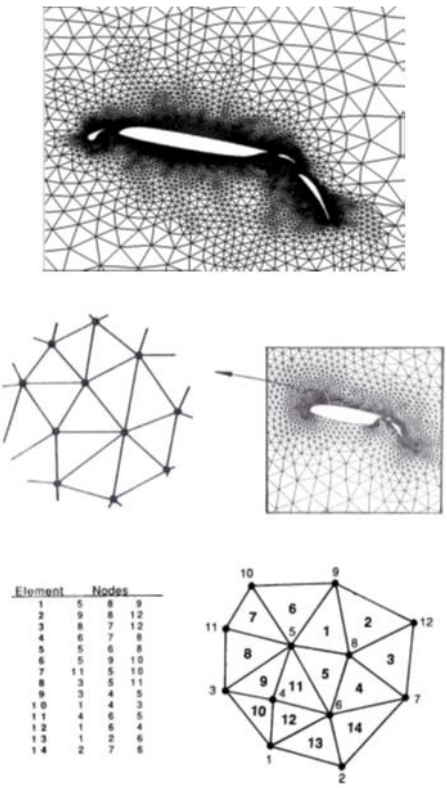

Figure 3.6 : Triangle mesh cell shape [19].

3.2.1.3 Mesh type implementation

There are many geometry combinations available in the study as shown in geometry chapter. Therefore different mesh types are also used in parallel with geometry. In the study of no inclination geometry, as the geometry is very easy to generate, structured mesh model is used at all mesh zones as seen Figure 3.8. Moreover, the mesh density between the outlet of jet nozzle and bottom wall area is much intenser than the other areas as the investigation points are in there.

There are two different number of mesh combination has tried for the solution as seen Figure 3.7. Due to low difference between 100 and 1000, the lower one is selected to continue the analysis faster. (Mesh size: 0.5 mm).The fully unstructured numerical mesh grid occurs about 280,000 quadrilateral cells. (Skewness=$1.3e^{-10}$ and $y^+ < 2.5$).

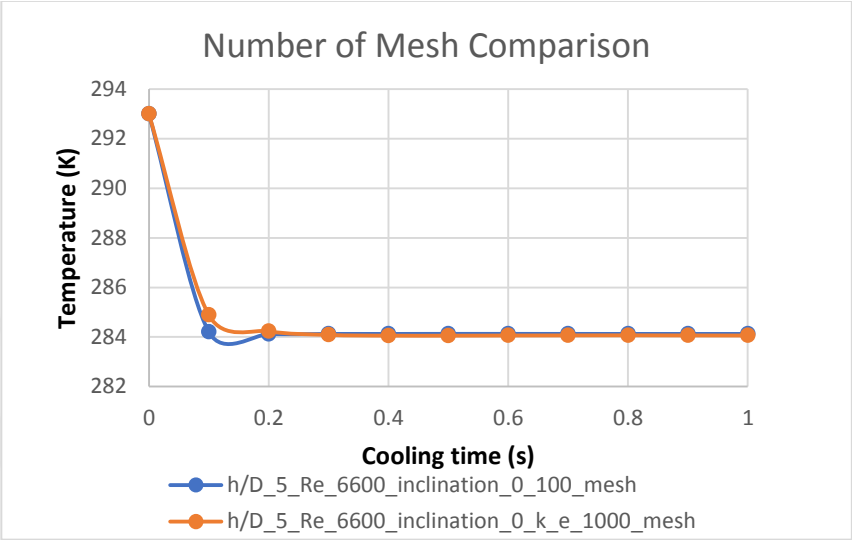

Figure 3.7 : Number of mesh comparison.

In the study of 10° & 20° inclination geometry, as the geometry is a little bit complicated to generate over no inclination study, structured and unstructured mesh model are use. Near the bottom wall side unstructured mesh is used while the other area is run with structured mesh. In addition to this, the mesh density between the outlet of jet nozzle and bottom wall area is much intenser than the other areas as the investigation points are in there just like no inclination study. (Element size: 0.5 mm). The partial unstructured numerical mesh grid occurs about 240,000 cells for 10° inclination as Figure 3.8. (Skewness=0.9 and $y^+ < 5$ normally <1.5)

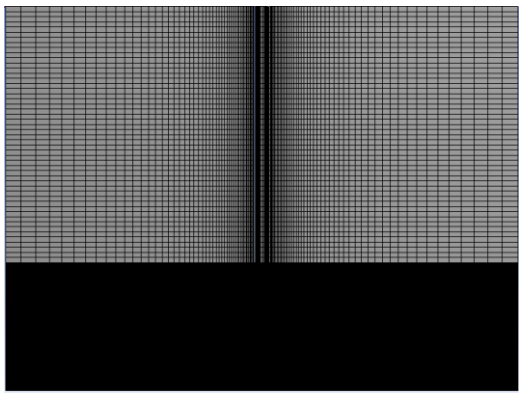

Figure 3.8 : Mesh study for the geometry with no inclination.

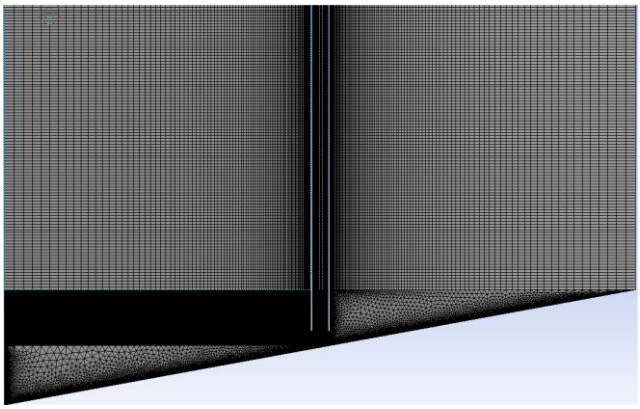

Figure 3.9 : Mesh study for the geometry with 10° inclination.

The partial unstructured numerical mesh grid occurs about 240,000 quadrilateral cells as Figure 3.9. (Skewness=0.92 and $y^+ < 5$)

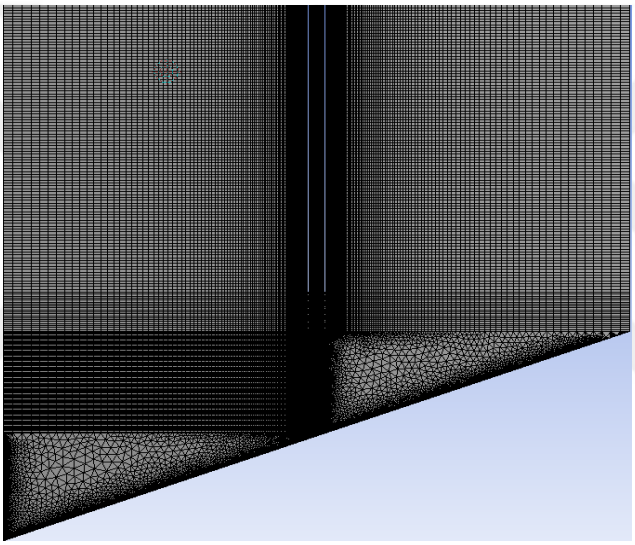

Figure 3.10 : Mesh study for the geometry with 20°inclination.

There is one more mesh study about geometry to see difference of structured and unstructured mesh type applied for inclination geometry as shown below Figure 3.10.

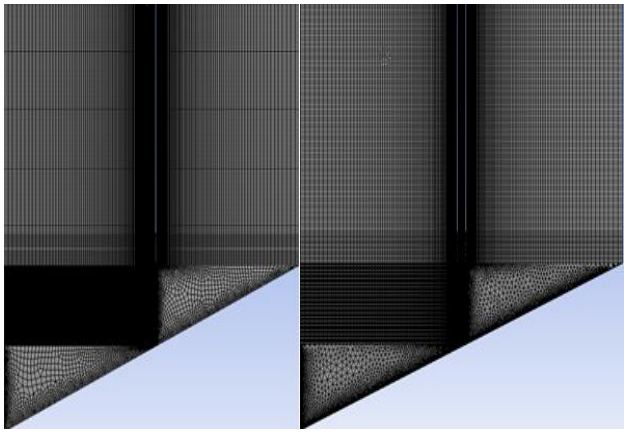

Figure 3.11 : Structured and unstructured mesh comparison at inclined area.

The results are expressed that there is no major difference between structured and unstructured mesh as shown below Figure 3.11.

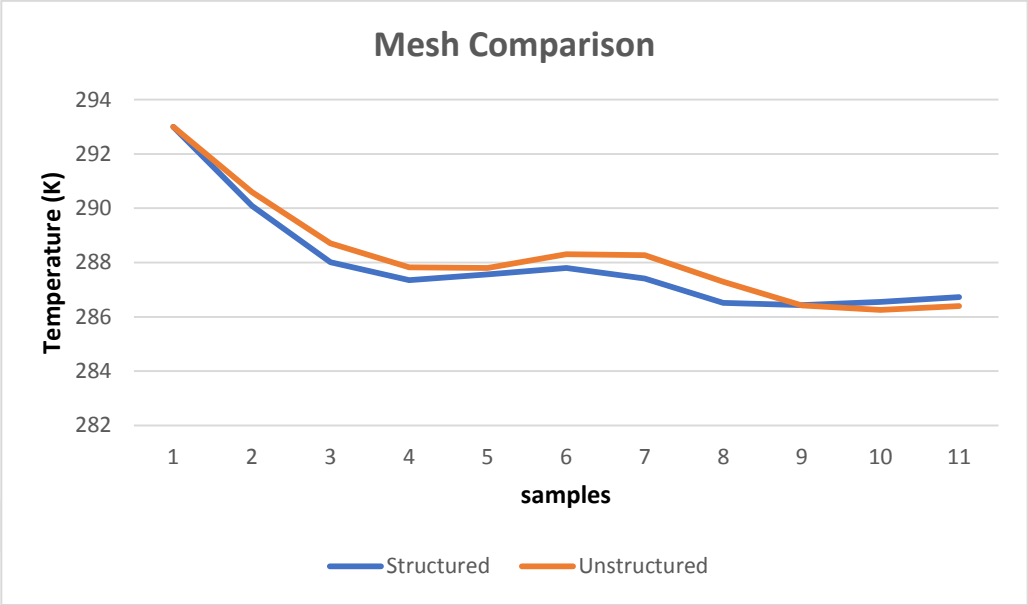

Figure 3.12 : Temperature comparison with structured and unstructured mesh type.

There is a mesh size named y_p requirement about SST k-w turbulent model which is used in one of three turbulent models for our study. Below calculations tells how to find it from C_f to Re correlation from equation 3.1 to 3.5.

$$Re = \frac{U_\infty \,.\, D}{\nu} \tag{3.1}$$

$$U_\infty = 5\frac{m}{s} \quad D = 0.01\ m \quad \nu = 1{,}5111.\ 10^{-5}\ @20\ \text{degree Celcius}$$

$$Re = \frac{5\ .0.01}{1{,}5111.\ 10^{-5}} = 3300$$

$$C_f = 0.0576\ .\ Re^{-1/5} \tag{3.2}$$

$$C_f = 0.0576\ .\ 3300^{-1/5} = 0.011$$

$$\zeta_w = 0.5\ .\ \rho\ .\ U_\infty .\ C_f \tag{3.3}$$

$$C_f = 0.011\ \ U_\infty = 5\frac{m}{s} \quad \rho = 1.2\ \frac{kg}{m^3}\ @20\ \text{degree Celcius}$$

$$\zeta_w = 0.5\ .\ 1.2\ .0.011.5 = 0.17$$

$$U_* = \sqrt{\frac{\zeta_w}{\rho}} \tag{3.4}$$

$$U_* = \sqrt{\frac{0.17}{1.2}} = 0.38$$

$$y_p = \frac{\nu \, . \, y^+}{U_*} \tag{3.5}$$

$$y^+ \leq 3$$

$$y_p = \frac{1{,}5111. \ 10^{-5} \, .3}{0.38} = 15 \, . 10^{-5} \, m$$

As mentioned before, the aim of the mesh size requirement is to capture the near bottom wall where the temperature and flow gradients were assumed to be highest flow conditions and increase the grid quality.

3.2.2 Set up

After geometry and suitable mesh selections, it is needed to arrange set up for the analysis.

In brief, the solution is pressure based and transient. Three of turbulent models are used for the comparison and there is one of them continued with the solution method. Boundary conditions are as given geometry section.

The following parts are about used equations & models for the study.

3.2.2.1 Governing equations

Below equations 3.6, 3.7 and 3.8 are three most important equations for the conservation of anything.

Therefore there are also applicable for the analysis performed.

Conservation of Mass

$$\frac{\partial \rho}{\partial t} + \nabla \cdot (\rho V) = 0 \tag{3.6}$$

Conservation of Energy (heat)

$$\frac{DvT}{Dt} = \frac{\partial T}{\partial t} + V \cdot \nabla T \tag{3.7}$$

Conservation of Momentum

$$\frac{\partial V}{\partial t} + (V \cdot \nabla)V = \frac{1}{\rho} \nabla \cdot \sigma + g \tag{3.8}$$

ρ : air density

P : total pressure

k : thermal conductivity

u : velocity

3.2.2.2 k-ε Turbulence models

There are 2 equation models used to see how the equations of turbulent kinetic energy (k) and deformation tensor (ε) are found and the viscosity is shown by taking k and ε. In this model, the deformation tensor equation includes a unit that does not have any chance to calculated at a wall function. For this reason, wall problems should be solved by using standart wall function model. In following titles, the standard and realizable k-ε models are shown due used them in the study with wall treatment [20].

Standard k-ε model

The model is which is has two equations semi-empirical model.The model is called possibly have the highest robustness, efficiency and most usage area. This turbulent model can be used and worked when the flow is totally turbulent and closer side of wall. About the Eddy model, one proposal suggests that turbulence consists of small eddies that are continuously forming and dissipating, and in which the Reynolds stresses are assumed to be proportional to mean velocity gradients. This defines an "eddy viscosity model". The model of this model is as follows from 3.9 equation to 3.13.

$$\mu_t = \rho \, . \, C_\mu \, \frac{k^2}{\varepsilon} \tag{3.9}$$

C_μ : experimental constant

$$\frac{\partial}{\partial t}(\rho k) + \frac{\partial}{\partial x_i}(\rho k U_1) = \frac{\partial}{\partial x_J}\left[(\mu + \frac{\mu_t}{\sigma_k})\frac{\partial k}{\partial x_j}\right] + P_k \quad (3.10)$$

$$\frac{\partial}{\partial t}(\rho \varepsilon) + \frac{\partial}{\partial x_i}(\rho \varepsilon U_1) = \frac{\partial}{\partial x_J}\left[(\mu + \frac{\mu_t}{\sigma_\varepsilon})\frac{\partial \varepsilon}{\partial x_j}\right] + C_{1\varepsilon}\frac{\varepsilon}{k}P_k - C_{2\varepsilon}\frac{\varepsilon^2}{k}\boldsymbol{\rho} \quad (3.11)$$

P_k : Turbulent kinetic energy

$$P_k = \mu_t . \bar{S}^2 \quad (3.12)$$

$\bar{S}$: Average of strain rate sensor in terms of time

$$\bar{S} = \sqrt{2 . \overline{S_{ij} S_{ij}}} \quad (3.13)$$

Finally, in order to use Standard k-ε Model, the constants should be;

$$C_{1\varepsilon} = 1.44$$

$$C_{2\varepsilon} = 1.92$$

$$C_\mu = 0.09$$

$$\sigma_k = 1$$

$$\sigma_\varepsilon = 1.3$$

Realizable k-ε model

The realizable k-ε Model is different from the standard k-ε model in two important ways:

- The Realizable k-ε model contains an alternative formulation for the turbulent viscosity.
- A modified transport equation for the dissipation rate, ε ,has been derived from an exact equation for the transport of the mean-square vorticity fluctuation.

The term “realizable” means that the model satisfies certain mathematical constraints on the Reynolds stresses, consistent with the physics of turbulent flows. The standard k-ε Model is not realizable.

The equation of the model is as follows from 3.14 equation to 3.20.

$$\frac{\partial}{\partial t}(\rho k) + \frac{\partial}{\partial x_i}(\rho k \bar{u}_i) = \frac{\partial}{\partial x_J}\left[(\mu + \frac{\mu_t}{\sigma_k})\frac{\partial k}{\partial x_j}\right] + P_k - \rho \cdot \varepsilon \quad (3.14)$$

$$\frac{\partial}{\partial t}(\rho\varepsilon) + \frac{\partial}{\partial x_i}(\rho\varepsilon U_i) \quad (3.15)$$

$$= \frac{\partial}{\partial x_J}\left[(\mu + \frac{\mu_t}{\sigma_\varepsilon})\frac{\partial \varepsilon}{\partial x_j}\right] + C_1 \cdot P_k \cdot S_\varepsilon - C_2 \cdot \frac{\varepsilon^2}{k + \sqrt{\vartheta \cdot \varepsilon}} \cdot \boldsymbol{\rho}$$

$$C_1 = \max\left[0.43, \frac{\eta}{\eta + s}\right] \quad (3.16)$$

$$C_\mu = \frac{1}{A_0 + A_s \cdot \frac{k \cdot U^*}{\varepsilon}} \quad (3.17)$$

$$U^* = \sqrt{S_{ij} \cdot S_{ij} + \widetilde{\Omega_{ij}\Omega_{ij}}} \quad (3.18)$$

$$A_0 = 4.04$$

$$A_s = \sqrt{6} \cdot \cos \boldsymbol{\Phi} \quad (3.19)$$

Finally, in order to use Realizable k-ε Model, the constants should be;

$$C_2 = 1.9$$

$$\sigma_k = 1$$

$$\sigma_\varepsilon = 1.2$$

3.2.2.3 k-ω Turbulence models

The K-omega model is one of the most commonly used turbulence models. It is a two equation model, that means, it includes two extra transport equations to represent the turbulent properties of the flow.

This allows a two equation model to account for history effects like convection and diffusion of turbulent energy. In this model, turbulent kinetic energy (k) and specific dissipation rate (w) are found. In following title, the SST k-ω model are shown due used them in the study with wall treatment.

SST *k-ω* Turbulence models

The SST k-ω model includes all the refinements of the BSL k-ω model, and in addition accounts for the transport of the turbulence shear stress in the definition of the turbulent viscosity. Menter (1994) is the first advised this model based on the complex of the standard k-ω model near the wall to a transformed k-ε model away from the wall. The equation of the model is as follows from 3.20 equation to 3.25.

$$\mu_t = \rho . \frac{k}{\boldsymbol{\omega}} . \frac{1}{\max[\frac{1}{a^*}, \frac{SF_2}{a_1 w}]} \tag{3.20}$$

$$\frac{\partial}{\partial t}(\rho . k) + \frac{\partial}{\partial x_i}(\rho . k . \bar{u}_i) \tag{3.21}$$

$$= \frac{\partial}{\partial x_J}[(\mu + \frac{\mu_t}{\sigma_k})\frac{\partial k}{\partial x_j}] + \min(P_k, 10 . \rho . \beta^* . k . w) - \rho . \beta^* . k . w$$

$$\frac{\partial}{\partial t}(\rho . w) + \frac{\partial}{\partial x_i}(\rho . w . \bar{u}_i) \tag{3.22}$$

$$= \frac{\partial}{\partial x_J}[(\mu + \frac{\mu_t}{\sigma_w})\frac{\partial w}{\partial x_j}] + a . \frac{w}{k} . P_k - \rho . \beta . w^2$$

$$\sigma_k = \frac{1}{\frac{F_1}{\sigma_{k,1}} + \frac{1 - F_1}{\sigma_{k,2}}} \tag{3.23}$$

$$\sigma_w = \frac{1}{\frac{F_1}{\sigma_{w,1}} + \frac{1 - F_1}{\sigma_{w,2}}} \tag{3.24}$$

$$\sigma_\infty = F_1 . \alpha_{\infty,1} + (1 - F_2) . \alpha_{\infty,2} \tag{3.25}$$

σ_w, σ_k : Prandtl numbers in terms of k and w

Finally, in order to use Realizable k-ε Model, the constants should be;

$$\sigma_{k,1} = 1.176$$

$$\sigma_{w,1} = 2$$

$$\sigma_{k,2} = 1$$

$$\sigma_{w,2} = 1.168$$

$$\sigma_1 = 0.31$$

$$\beta_{i,1} = 0.075$$

$$\beta_{i,2} = 0.0828$$

3.2.3 Comparison of turbulent models

For the comparison of turbulent model by using circular jet shape,the design with parameters of Re = 6,600, D = 10 mm and H/D = 5 are first considered as a comparison for validation. The bottom wall temperature distribution and the average temperature of bottom wall as a function of cooling time are numerically simulated by using three different turbulent models. For the suitable mesh size calculation, there is a mesh size named y_p requirement about SST k-w turbulent model which is used in one of three turbulent models for the study. After obtaining required minimum mesh size (y_p) from C_f to Re correlation, the value of it is used for all turbulent models comparison to get under the same conditions. Figure 3.12 helps to see the turbulent model comparison between numerical results at Re = 6,600 and H/D = 5. According to the comparative analysis of three different turbulent models, it can be seen that the turbulent models give almost the same results with respect to cooling time. Considering results with this perspective, the standart wall function k-ε turbulence model is selected as suitable turbulent model for all of the simulations.

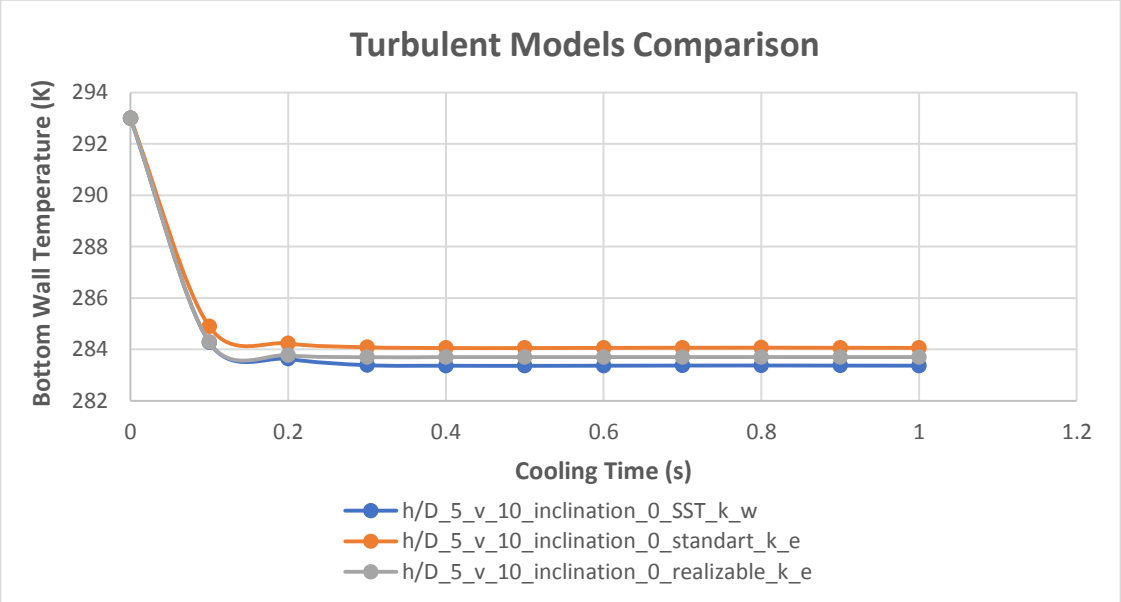

Figure 3.13 : Turbulent model comparison.

4. RESULTS AND DISCUSSION

4.1 Overview

As mentioned before, the study is about to investigate the influence of key facts that effect the cooling performance of jet impingement system in four main subjects to determine the predominant approach. The jet nozzle flow type which is get from two different inlet velocity of jet, the distance between the bottom wall and jet nozzle outlet, bottom wall surface inclination and the blockage on the way of jet flow. Jet impingement under the transient case, the observation is useful to investigate on air impinging jets for transient heat transfer characteristics under simulation of between low of jet nozzle and plate distances and less temperature differences between the jet nozzle inlet and bottom wall. The related study is carried out with two different Reynolds number (Re) in the range of 3,000 to 6,000 which are got from two different jet nozzle inlet velocity 5 and 10 m/s under the same circular diameter of small jet with 10 mm. The jet flows can be evaluated with turbulent flow according to Reynold numbers and the solution methods are based on this evaluation. The other effect that the ratio of the jet nozzle and bottom wall distance (H) and the jet nozzle diameter (D) which is H/D changes as 1 & 5 &10. In addition to these, the inclination of bottom surface (α) which is projected to be an important role for the cooling profile is as no slope & 10° & 20°. Lastly, the circular blockage effect on the flow is investigated.

There are many simulations run for finding the efficient set up as shown Figure 4.1. For various combination of the ratio of the distance between jet nozzle and bottom wall (H) and the constant diameter of jet nozzle (D=10 mm) which is H/D, Reynolds number (Re) which is affected from the just inlet velocity variation of jet nozzle as the temperature of the air at jet inlet and the diameter of jet nozzle is constant, the inclination (α) which inspires us the design of plate and the blockage effect, the distribution of average bottom wall temperature specify according to cooling time are seen in Figure 4.1.

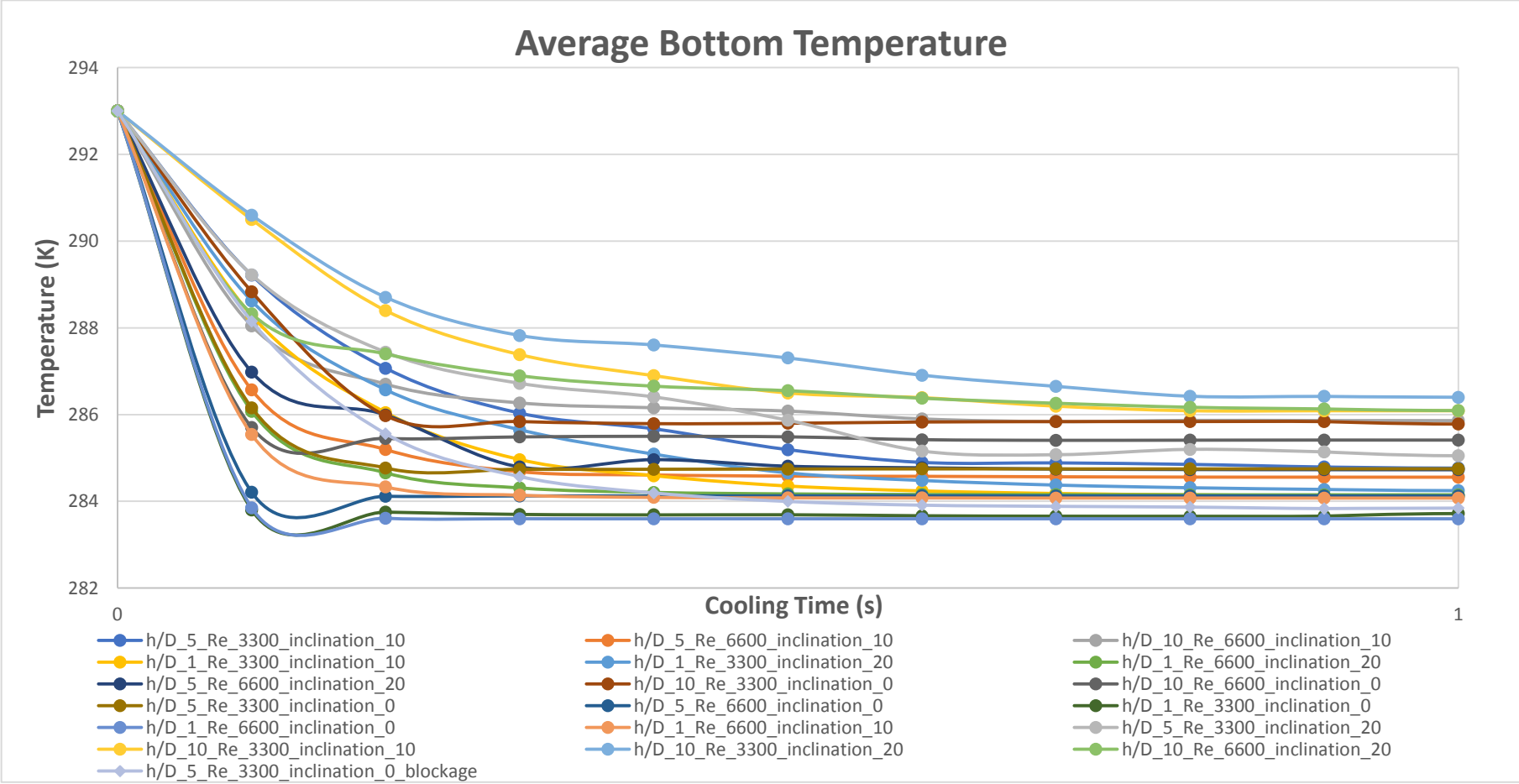

Figure 4.1 : Average bottom temperature for all simulations.

There are many simulations run for finding the efficient set up as shown Figure 4.1. For various combination of the ratio of the distance between jet nozzle and bottom wall (H) and the constant diameter of jet nozzle (D=10 mm) which is H/D, Reynolds number (Re) which is affected from the just inlet velocity variation of jet nozzle as the temperature of the air at jet inlet and the diameter of jet nozzle is constant, the inclination (α) which inspires us the design of plate and the blockage effect, the distribution of average bottom wall temperature specify according to cooling time are seen in Figure 4.1. As seen from the Figure 4.1, total cooling time is accepted 6 seconds for all simulations since it is enough time to see the effect for air according to below calculations. In other words, we can have a chance to see the effect of air on the bottom wall temperature easily because the observation time for 5 m/s inlet velocity set up is 150 times longer than the total time air passes through the jet nozzle. In parallel with 5 m/s, investigation time for 10 m/s is 300 times longer than the time air passes through the jet nozzle. As a result of this in worst case the time is sufficient to evaluate and see the conditions of air flow. To find how long the air takes to pass from the beginning of the jet nozzle to end as equation 4.1

L = 200 mm

V= 5 & 10 m/s

$$X = V \,.\, t \tag{4.1}$$

$$200 \,.\, 10^{-3} = 5 \,.\, t_1$$

$$t_1 = 0{,}04\ s$$

$$200 \,.\, 10^{-3} = 10 \,.\, t_2$$

$$t_2 = 0{,}02\ s$$

In the study, the temperatures are taken close to each other to observe temperature behaviour under small temperature differences. It is taken that the initial temperature of jet inlet is 283 degree K while the bottom wall temperature is 293 degree K. From the cooling profile in the Figure, the average bottom wall temperature drops quickly to in the range of 284-286 degree K nearly for all simulations.

The first quick cooling time takes almost two & three times shorter than the time which the temperature in the every study is getting steady condition.

The reason of this time difference can be explained as the more temperature differences, the shorter time the beginning temperature balanced. And in addition to that, while the cooling time range is the same, the rate of temperature decrease continually drops with time of 0.5 seconds and after this second, the temperatures are getting steady as the heat transfer between jet and bottom wall is in balanced.

4.2 Reynolds Number Effect on Average Bottom Temperature

The simulation results for different Reynolds number when no inclination and various H/D ratio conditions, the temperature situation is as Figure 4.2, Figure 4.3 and Figure 4.4.

As seen all below figures, when the velocity of nozzle inlet is higher which means Reynolds number of it is higher, the cooling time is shorter and the balanced temperature is lower. From Figure1 which is shown lower H/D ratio, the cooled temperature can be said almost the same while the cooling profile difference is apperant in the simulation with higher H/D ratio.

Furthermore, it is certain that with the increase of H/D ratio, thermic neutrality temperature of the bottom is getting higher as the effect of jet flow influence on the bottom temperature is is decreased due to high distance between bottom wall and jet nozzle. To give an example, the equilibrium bottom wall temperature of Figure 4.2 is about 284°K whereas Figure 4.4 which is higher H/D ratio is nearly 286°K.

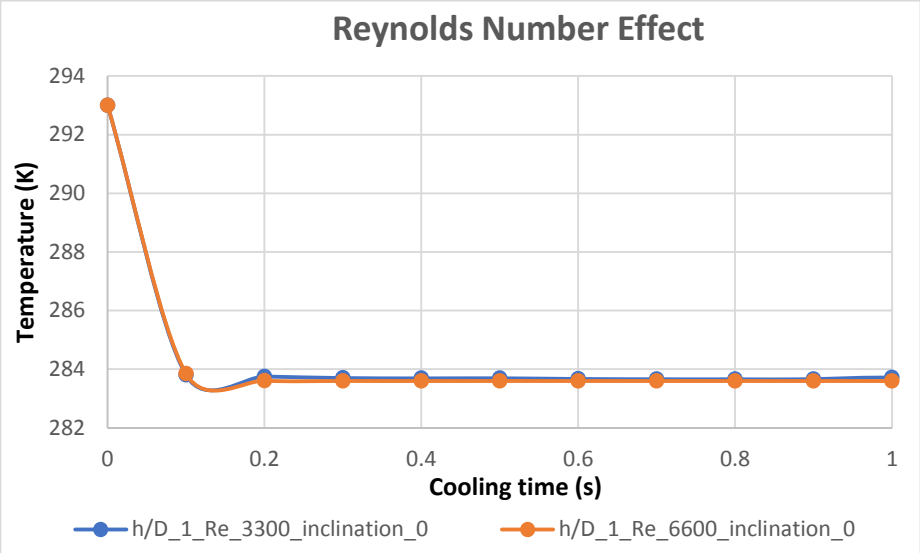

Figure 4.2 : Cooling profile and time comparison at low H/D ratio and no inclination.

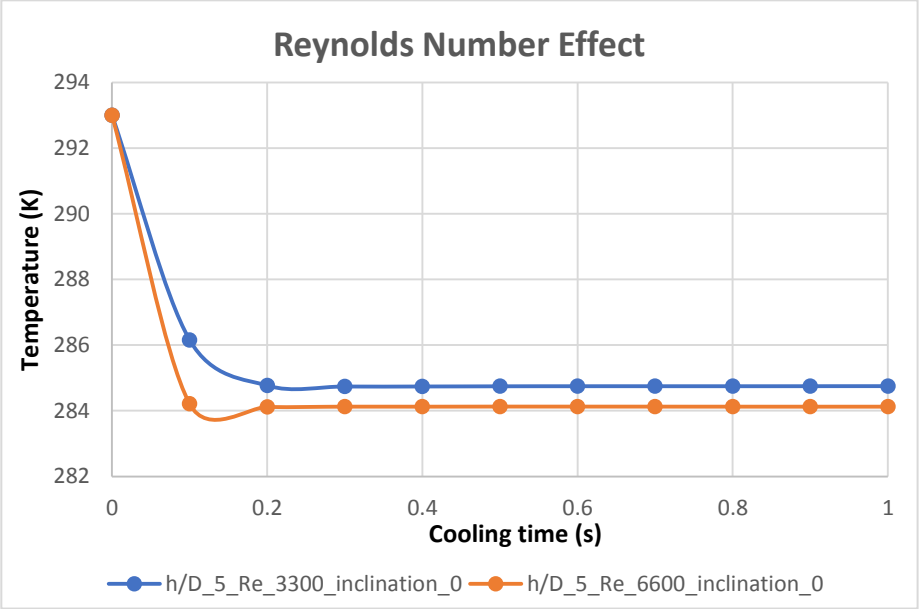

Figure 4.3 : Cooling profile and time comparison at medium H/D ratio and no inclination.

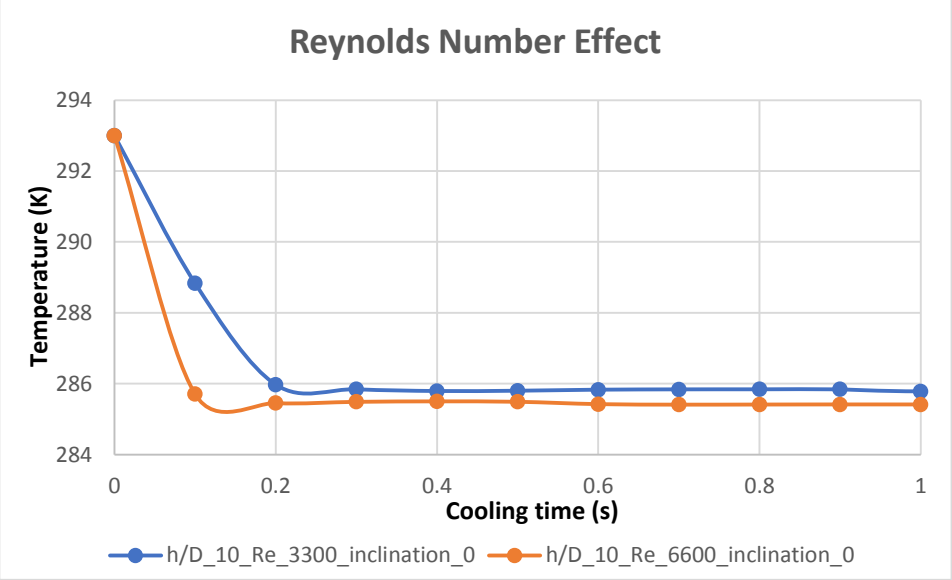

Figure 4.4 : Cooling profile and time comparison at high H/D ratio and no inclination.

The below figures are about different Reynolds number when 10° inclination and various H/D ratio conditions, the temperature situation is as Figure 4.5, Figure 4.6 and Figure 4.7.

As seen the figures, the same situation is observed for 10° inclination looking no inclination. The cooling time is longer and the balanced temperature is higher if the Reynolds number is smaller . And the finding the balancing temperature takes longer time than no inclination condition.

From Figure 4.5 with lower H/D ratio, the balanced temperatures are nearly the same.

Moreover, the balanced temperatures are getting lower when H/D ratio is smaller.

To give an example, the equilibrium bottom wall temperature of Figure 4.5 is about 284°K whereas Figure 4.7 which is higher H/D ratio is nearly 286°K.

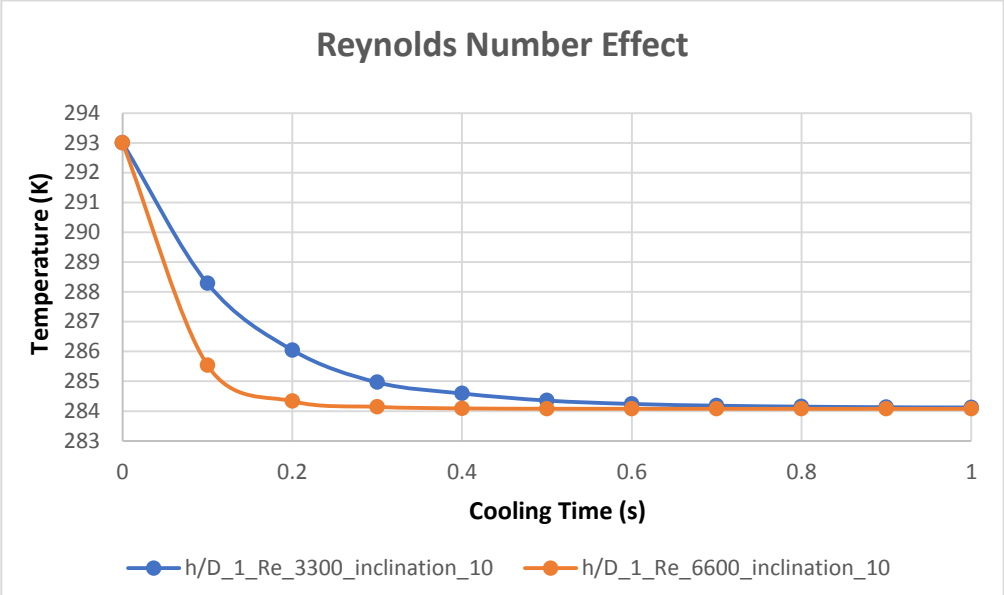

Figure 4.5 : Cooling profile and time comparison at low H/D ratio and 10° inclination.

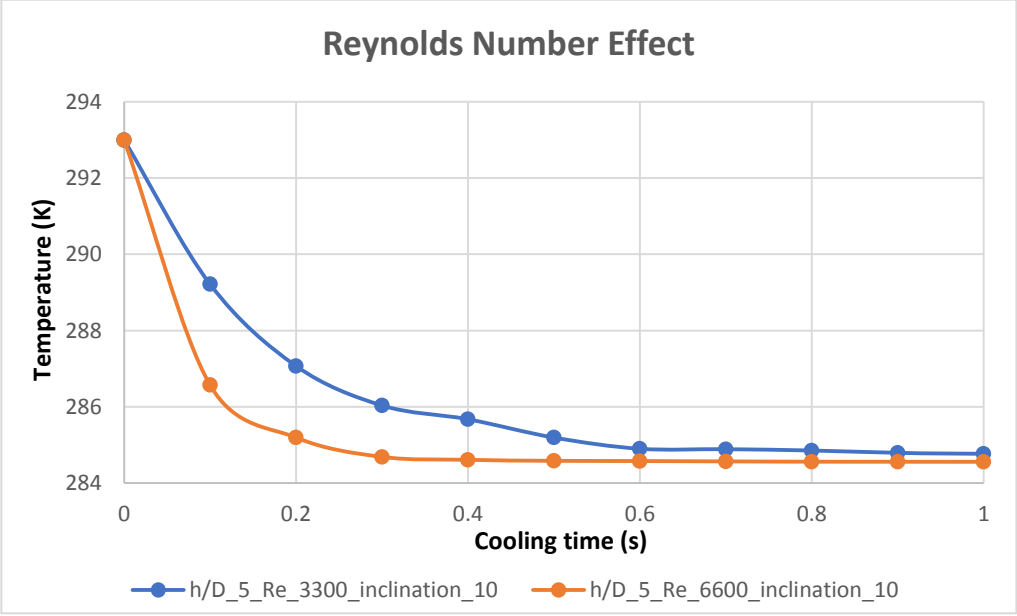

Figure 4.6 : Cooling profile and time comparison at medium H/D ratio and 10° inclination.

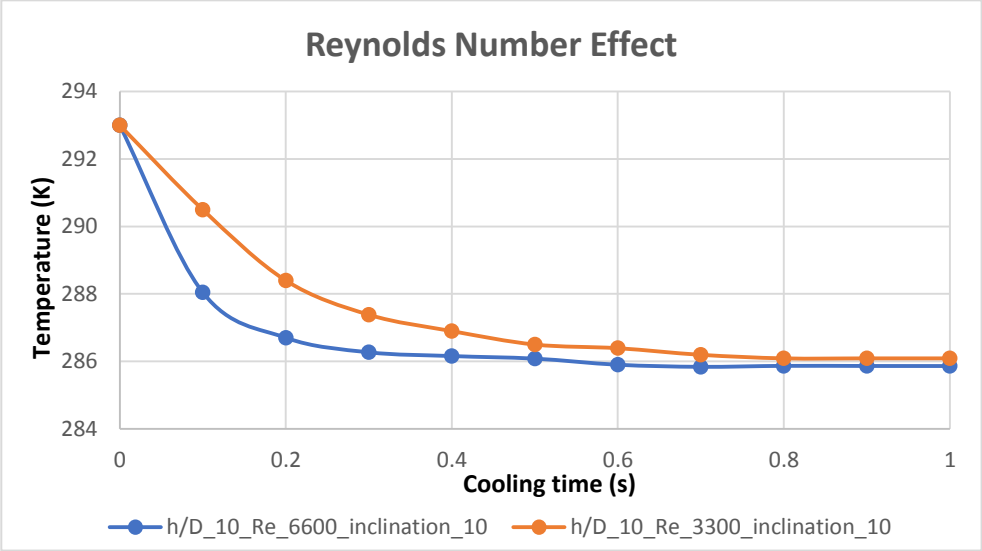

Figure 4.7 : Cooling profile and time comparison at high H/D ratio and 10° inclination.

These are related different Reynolds number when 20° inclination and various H/D ratio conditions, the temperature conditions are as Figure 4.8, Figure 4.9 and Figure 4.10. From the figures, the results are the same as no and 10° inclination. The cooling time and the balanced temperature are inversely proportional of Reynolds number magnitude. In addition, getting balancing temperature takes longer time than no and 10° inclination condition.

In addition to this, the values of balanced temperatures are directly proportional of H/D ratio. For example, the equilibrium bottom wall temperature of Figure 4.8 is about 284°K whereas Figure 4.10 where is higher H/D ratio is nearly 286°K.

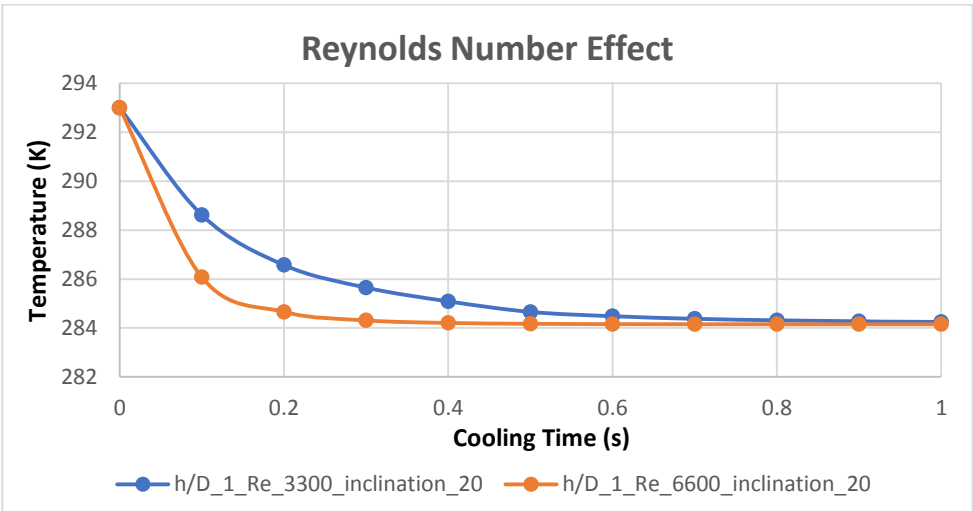

Figure 4.8 : Cooling profile and time comparison at low H/D ratio and 20° inclination.

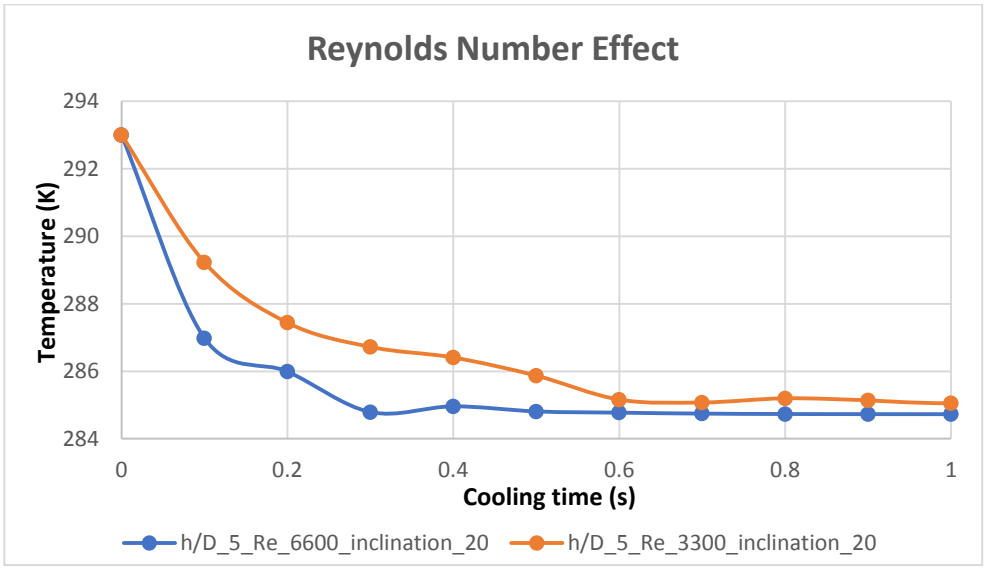

Figure 4.9 : Cooling profile and time comparison at medium H/D ratio and 20° inclination.

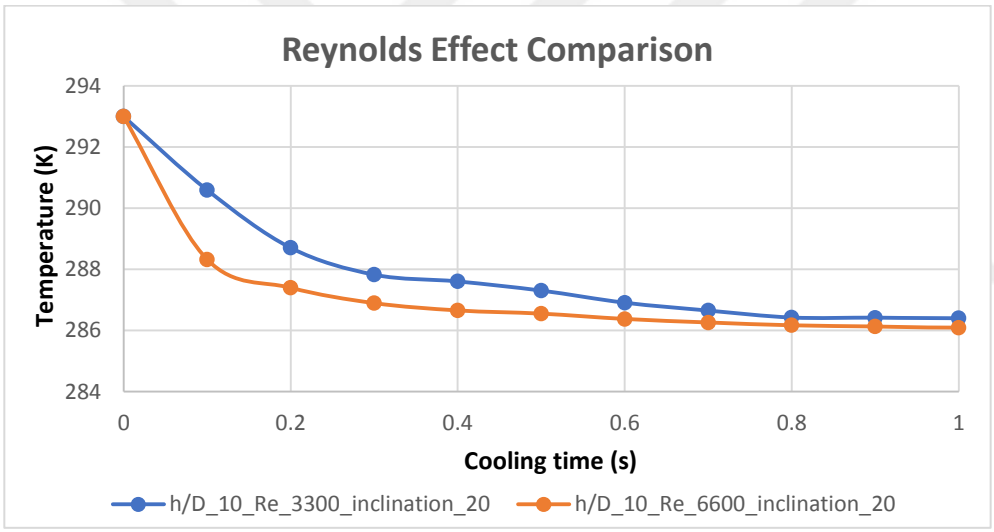

Figure 4.10 : Cooling profile and time comparison at high H/D ratio and 20° inclination.

4.3 H/D Ratio Effect on Average Bottom Temperature

The simulation results for different H/D ratio when constant Reynolds number of 3300 and various inclinations, the temperatures are like Figure 4.11, Figure 4.12 and Figure 4.13.

As seen all below figures, when distance between bottom wall and jet nozzle (H) become higher which means H/D ratio of it is higher, the cooling time is longer and the balanced temperature is lower.

Furthermore it is obvious that with the increase of inclination, thermic neutrality temperature of the bottom is getting a little bit higher than the other inclination study since the effect of jet flow on the bottom temperature is decreased due to nonuniform flow distribution.

To give an example, the equilibrium bottom wall temperature of Figure 4.11 for H/D ratio 1 is about 284°K whereas figure 4.13 which is higher inclination is a little bit more than 284°K.

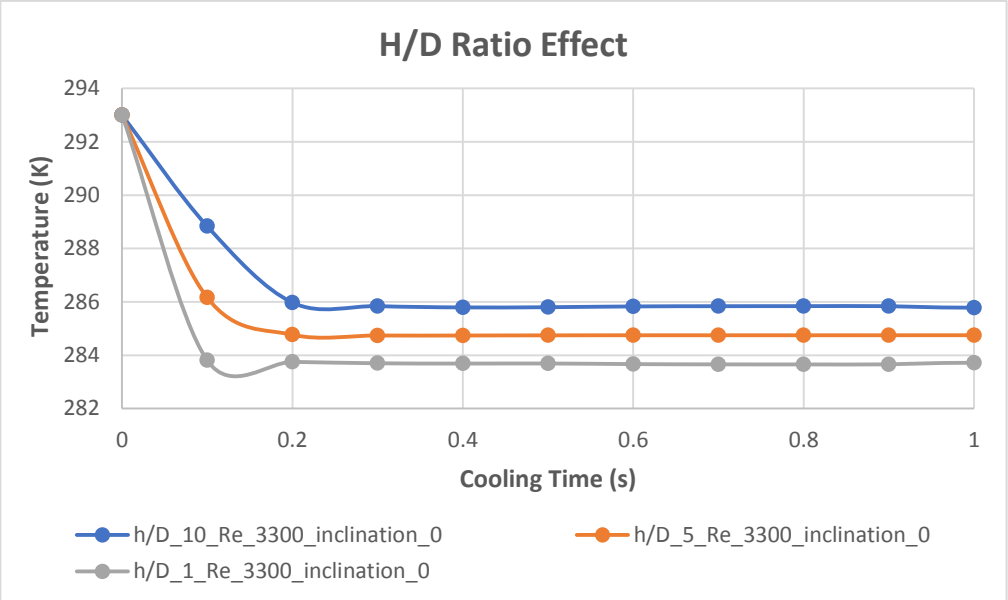

Figure 4.11 : Cooling profile and time comparison at low Reynolds number and 0° inclination.

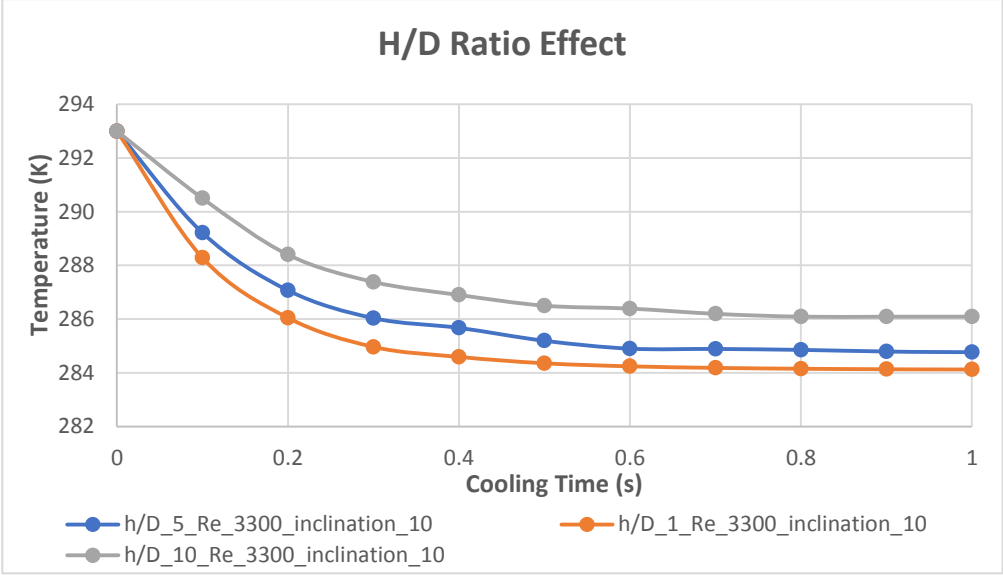

Figure 4.12 : Cooling profile and time comparison at low Reynolds number and 10° inclination.

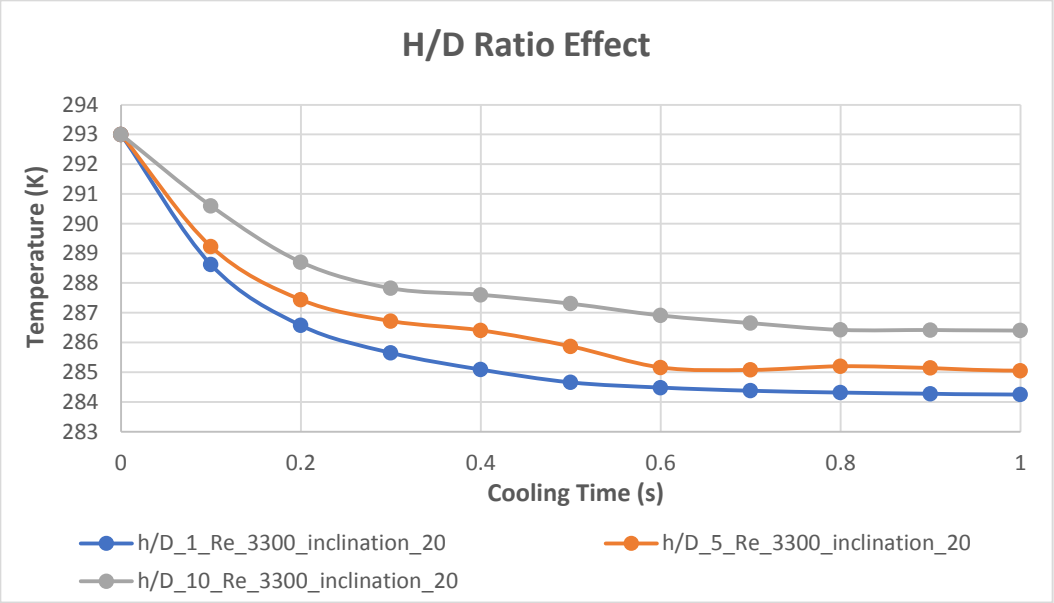

Figure 4.13 : Cooling profile and time comparison at low Reynolds number and 20° inclination.

The below figures are about different H/D ratio when Reynolds number of 6600 and various inclinations, the temperature situation is as Figure 4.14, Figure 4.15 and Figure 4.16. As seen the figures, the same situation is observed for 10° inclination looking no inclination. The cooling time is shorter and the balanced temperature is lower if the H/D ratio is smaller. Moreover, the irregular flow due to inclination causes higher balanced temperature. For example, the equilibrium bottom wall temperature of Figure 4.14 for H/D ratio 10 is a little bit lower than 286°K whereas Figure 4.16 which is higher inclination is about 286°K.

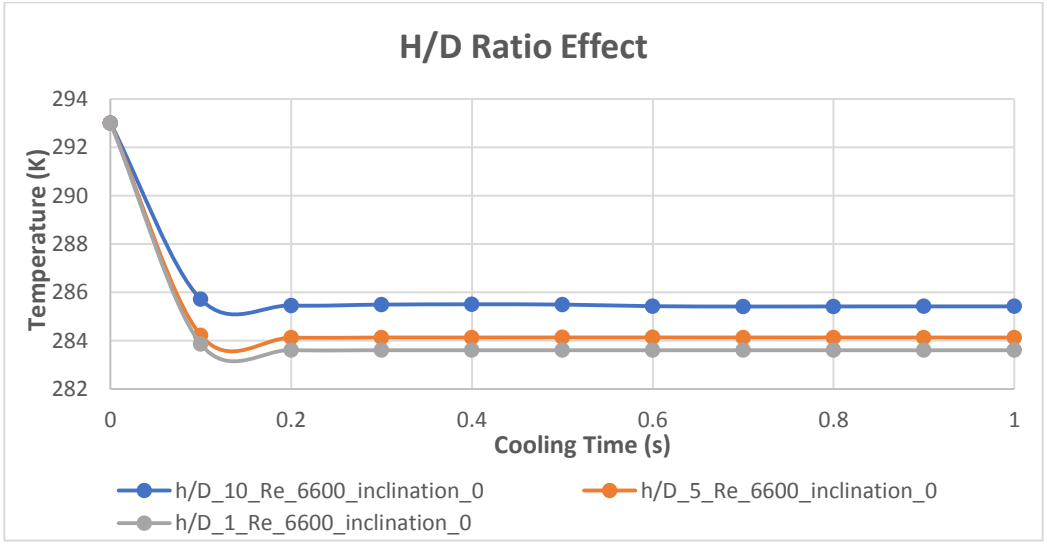

Figure 4.14 : Cooling profile and time comparison at high Reynolds number and 0° inclination.

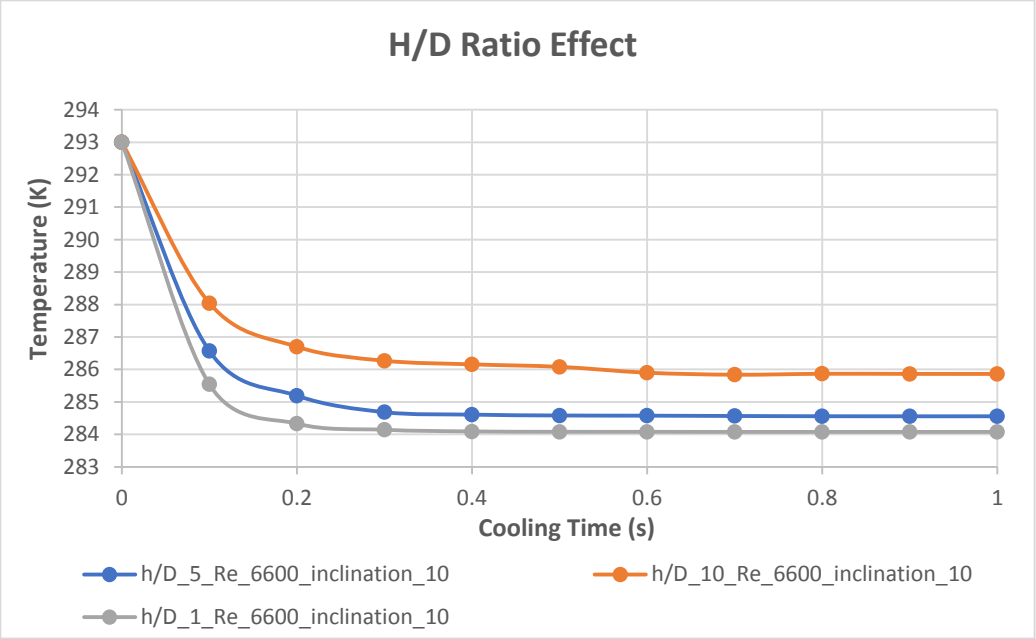

Figure 4.15 : Cooling profile and time comparison at high Reynolds number and 10° inclination.

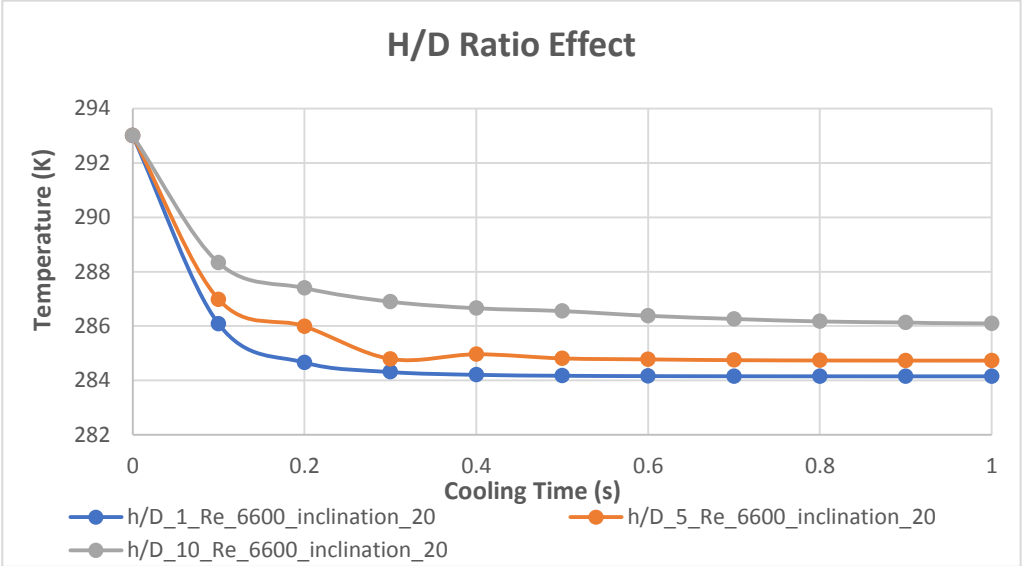

Figure 4.16 : Cooling profile and time comparison at high Reynolds number and 20° inclination.

4.4 Inclination Effect on Average Bottom Temperature

The simulation results for different inclinations when constant Reynolds number of 3300 and various H/D ratio, the obtained temperatures are just like Figure 4.17, Figure 4.18 and Figure 4.19. As seen all below figures, when inclination of bottom wall temperature is getting higher which means α of it is higher, the cooling time is longer and the balanced temperature is higher.

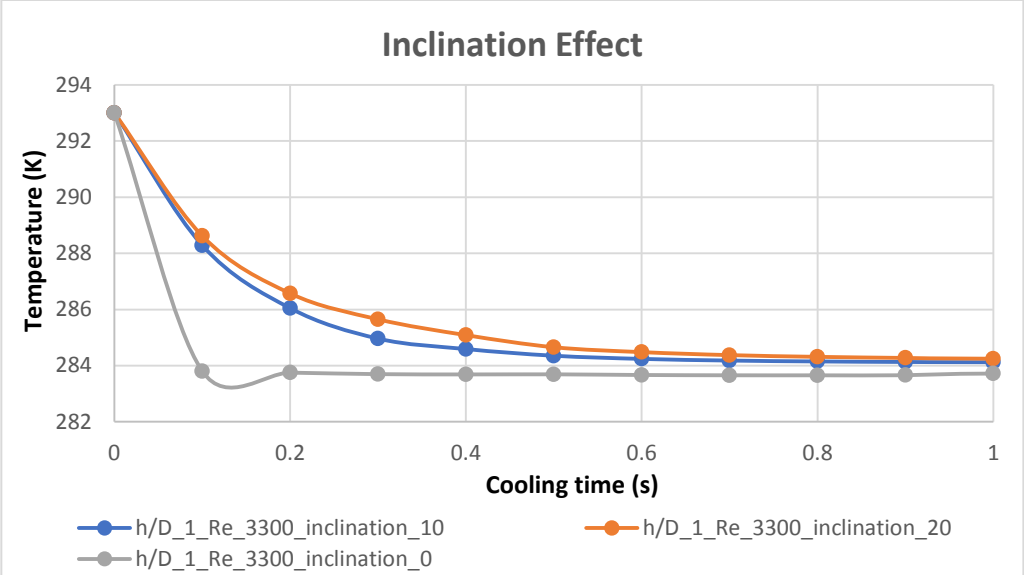

Figure 4.17 : Cooling profile and time comparison at low Reynolds number and H/D ratio.

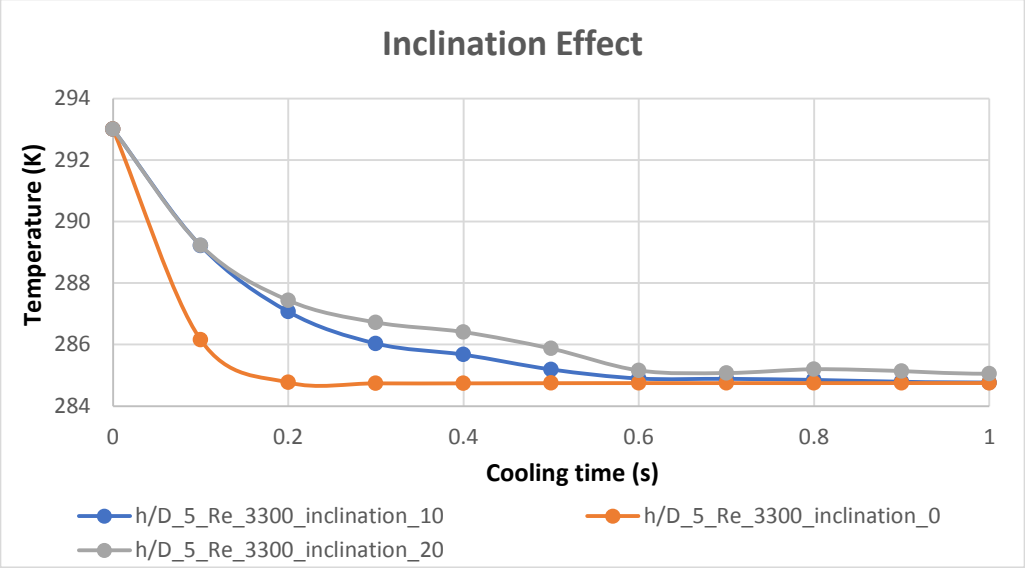

Figure 4.18 : Cooling profile and time comparison at low Reynolds number and medium H/D ratio.

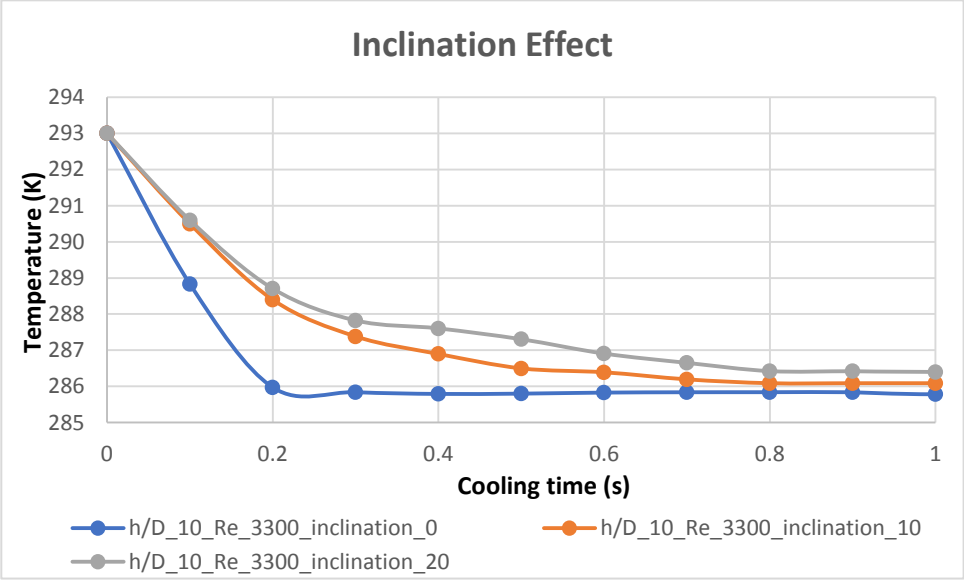

Figure 4.19 : Cooling profile and time comparison at low Reynolds number and high H/D ratio.

These are related different inclinations when Reynolds number with 6600 and varied H/D ratio, the temperature conditions are as Figure 4.20, Figure 4.21 and Figure 4.22.

From the figures, the results are in parallel with Reynolds number with 3300. The cooling time and the balanced temperature are directly proportional of inclination value. And getting balancing temperature with higher H/D takes longer time than the lower H/D results.

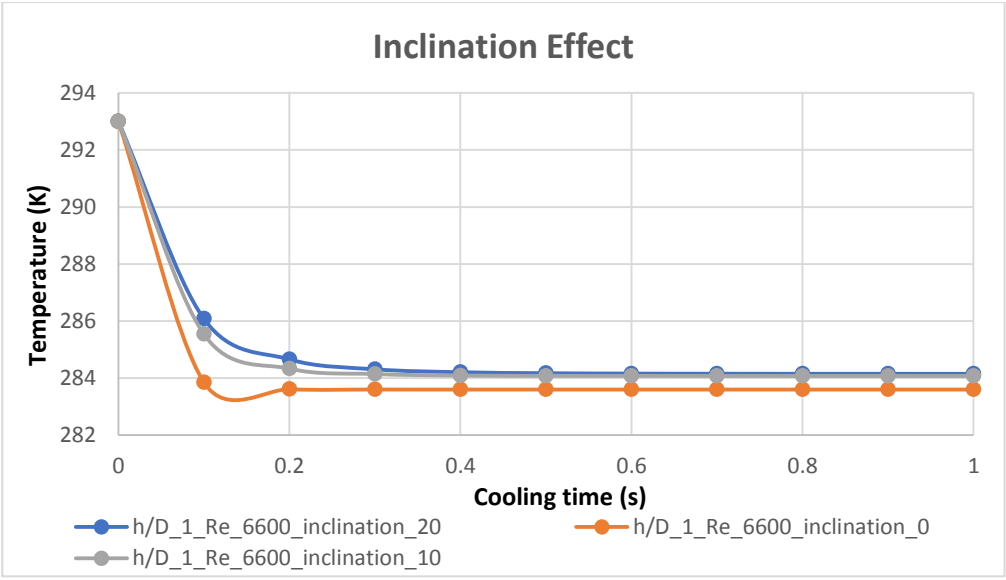

Figure 4.20 : Cooling profile and time comparison at high Reynolds number and low H/D ratio.

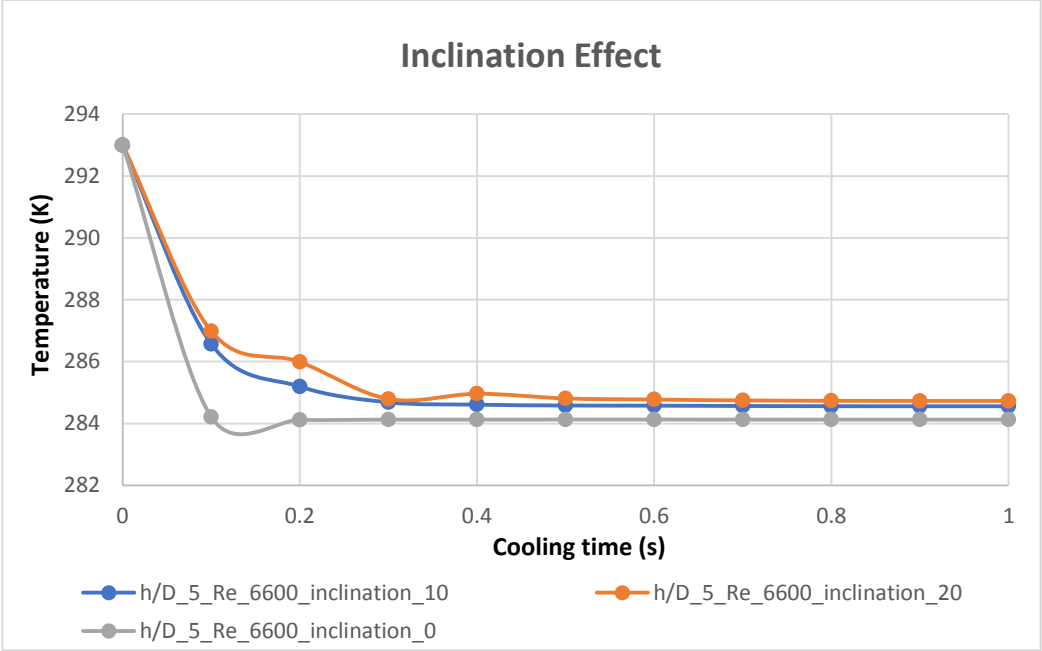

Figure 4.21 : Cooling profile and time comparison at high Reynolds number and medium H/D ratio.

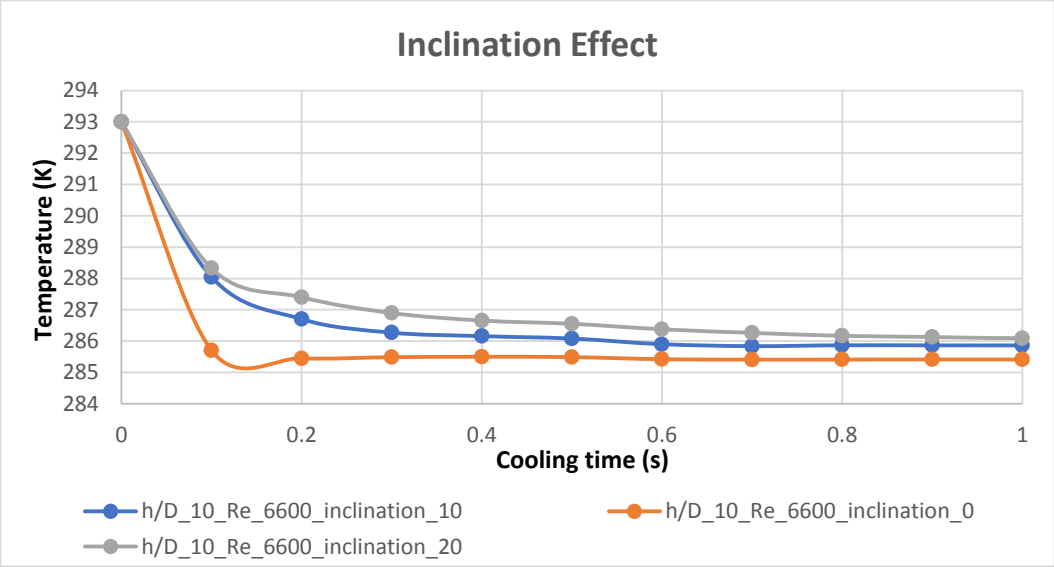

Figure 4.22 : Cooling profile and time comparison at high Reynolds number and H/D ratio.

Furthermore it is very clear that with the increase of Reynolds number, thermic neutrality temperature of the bottom is getting a little bit lower since the effect of heat transfer on the bottom temperature is increased due to higher velocity. To give an example, the equilibrium bottom wall temperature of Figure 4.18 for Reynolds number 3300 is about 285°K whereas Figure 4.21 which is higher Reynolds number is almost 284°K.

Finally, as it can be understood from all of the inclination effect comparison figures, when the inclination (α) is low, the final temperatures of the bottom wall is also low. To analyse why it is like this, the below study which compares ended temperatures of the location of points at the bottom wall is happened.

The results tell us the temperatures at the negative side are higher than the positive side due to pressure effect. The total pressure is lower at positive side due to geometry according to Figure 4.24. Therefore the flow prefers to pass to low pressure area the flow distribution and is getting non uniform and causes different temperature distribution as seen below Figure 4.23.

On the other hand the cooling profile is similar in everywehere when no inclination is occurred since the pressure distribution is uniform as shown Figure 4.25.

The reason of temperature difference between inclination complexity can be explained clearly with this study.

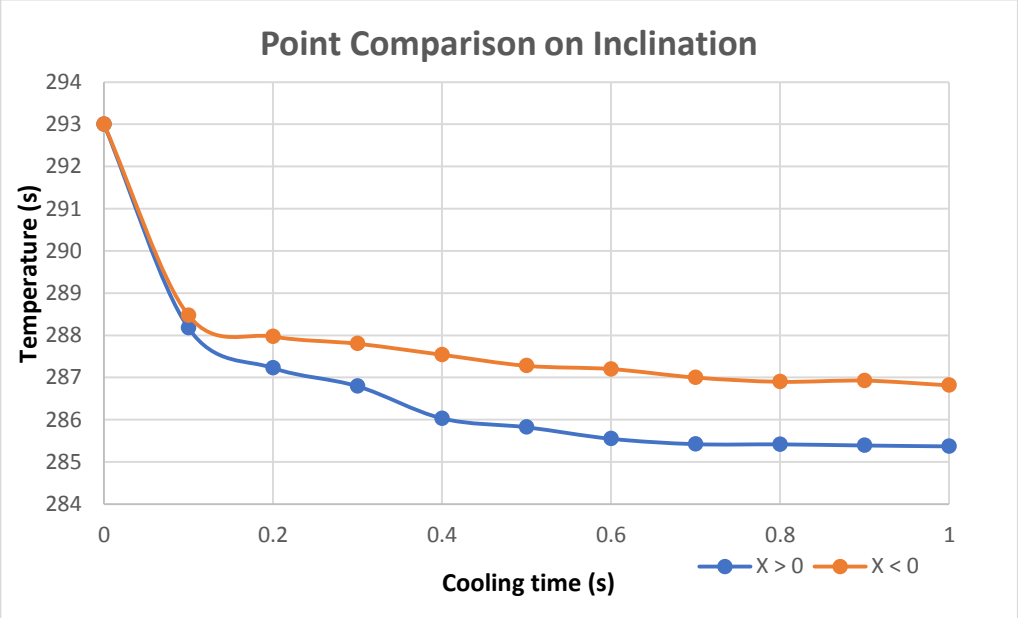

Figure 4.23 : Average temperature of locations of bottom wall at high H/D ratio and 20° inclination.

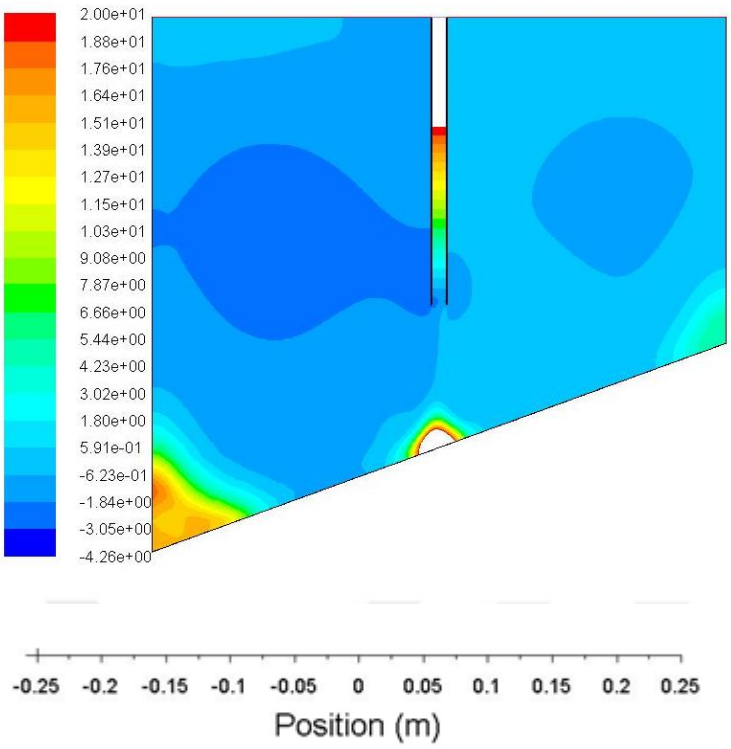

Figure 4.24 : Pressure distribution of the 20° inclination.

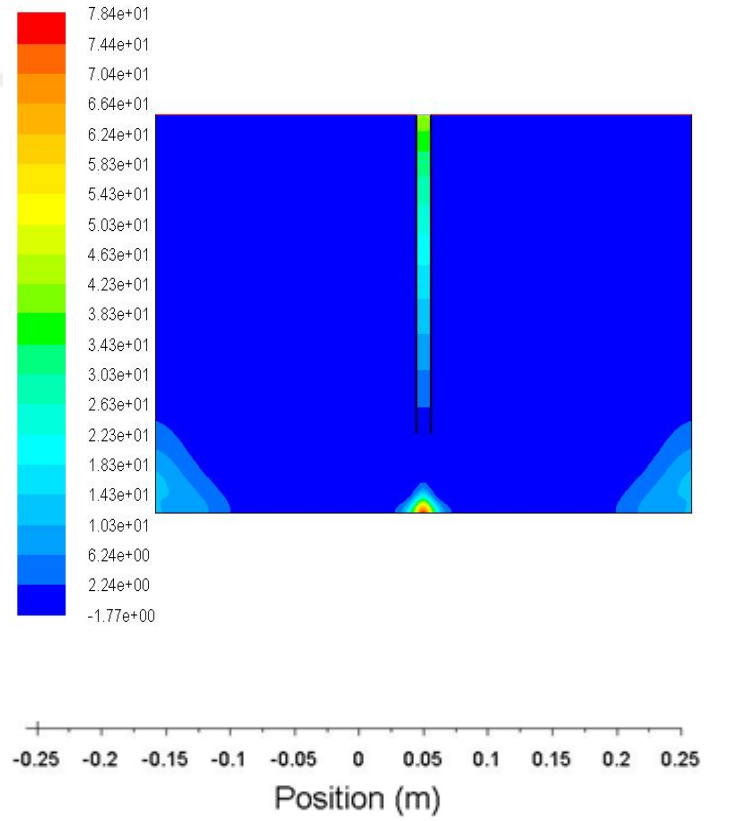

Figure 4.25 : Pressure distribution of the no inclination.

4.5 Blockage Effect on Average Bottom Temperature

The Figure 4.24 is relevant with blockage effect on the bottom temperatures when under no inclination, H/D ratio with 5 and Reynolds number of 3300 conditions, the temperature conditions. From the Figure 4.25, putting a blockage to on the way of flow makes contribution to cools the bottom wall temperature more while the cooling period of it is more slowly in early seconds. In brief, if the quick cooling is desired, blockage is not a good idea. However, in contrast with it, if the colder temperature is desired indepedently of time, blockage should be used.

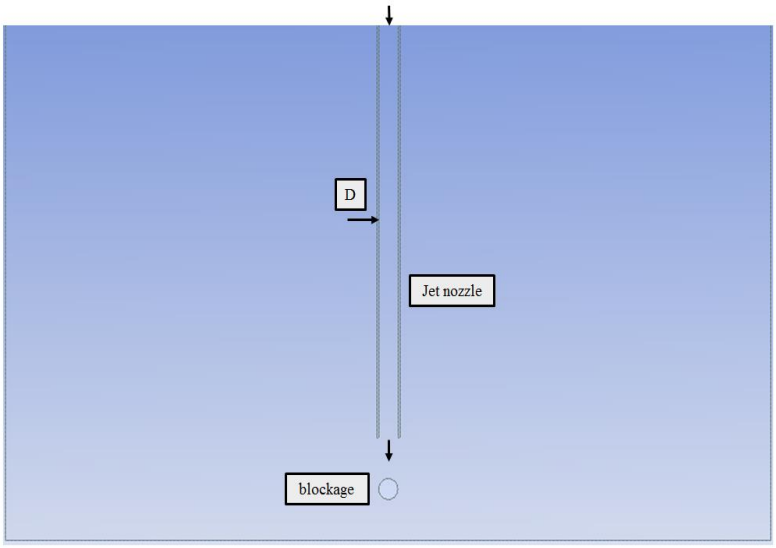

Figure 4.26 : The geometry with blockage.

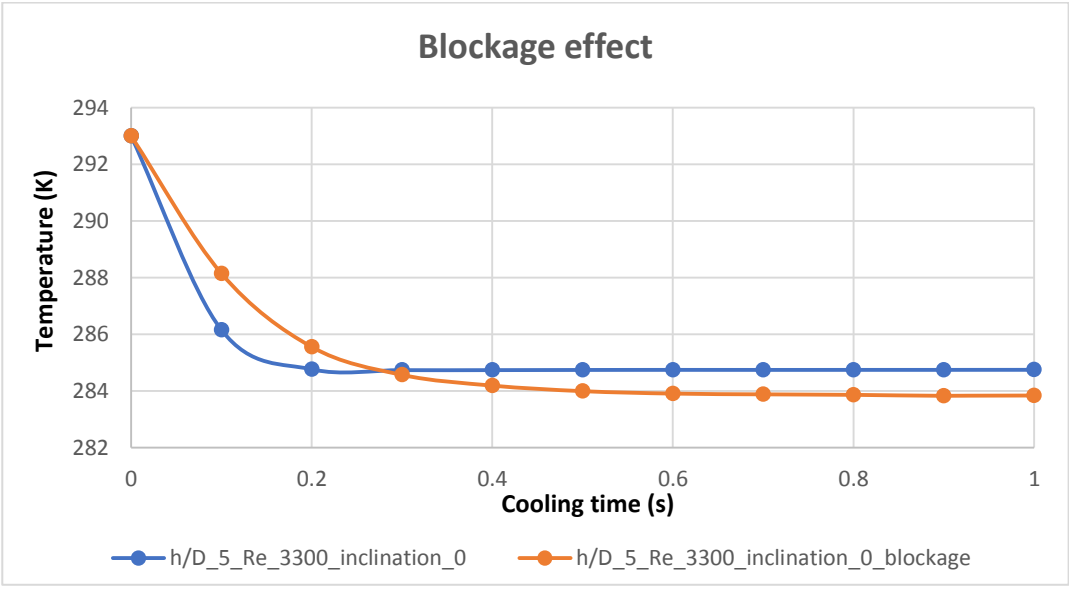

Figure 4.27 : Cooling profile and time comparison in terms of blockage.

To sum up with using all simulations, as shown in Figure 4.26, with the conditions of more H/D ratio and inclination, the less the Re, the longer the quenching time and higher final temperature. Blockage effect is estimated to pull the temperatures down by using previous Figure. Therefore, minimum H/D ratio, inclination, maximum inlet velocity with the blockage can be said the best configuration.

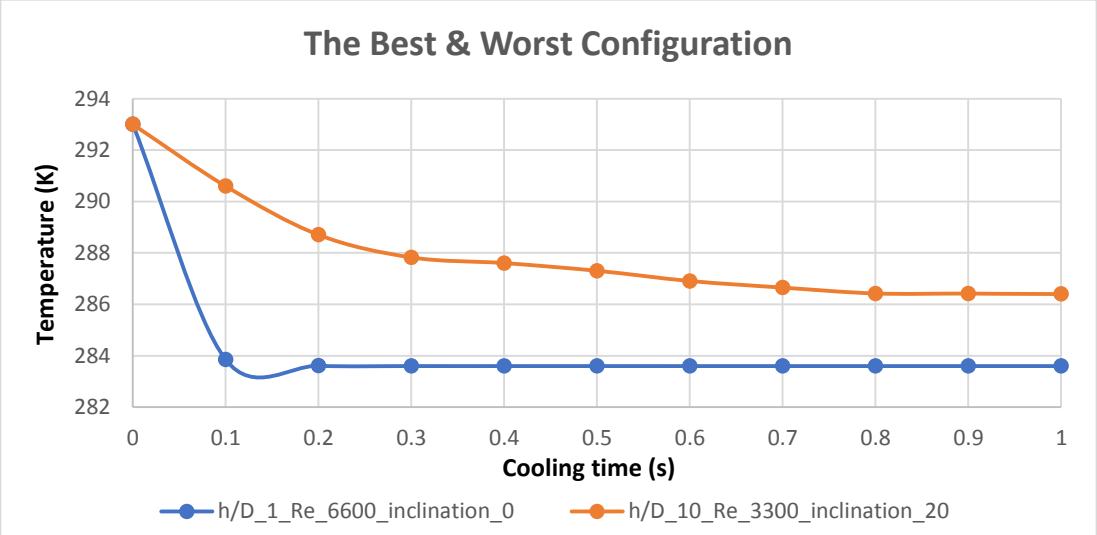

Figure 4.28 : The best and worst design comparison with regard to cooling profile and time.

5. CONCLUSION

In this study, to examine the transient heat transfer characteristics of air impinging jets under conditions of between small jet plate distances and low temperature differences between the inlet and bottom wall of sizes with 400 mm were achieved numerical methods.The inlet velocity of jet nozzle with different Reynolds number (Re), the ratio of the distance between outlet of circular jet and the bottom wall (H) and nozzle diameter (D) (H/D), bottom surface inclination and the blockage are variable inputs to get the efficient cooling profile. For this cause, variations of transient temperature characteristics of the bottom wall surface depending on cooling times were observed in depth.

It is concluded that all of the inputs which are observed have significant effect on the temperature of the bottom wall surface. The effects are mentioned in the following sections. When investigated Reynolds effect on the average bottom temperature, the average temperatures are getting lower as the Reynolds number is increased by rising velocity of inlet jet nozzle. The cooling time becomes shorter due to this reason as well. As is known, the velocity increase causes Nusselt number raise and the heat transfer performance is improved thanks to velocity directly.The studies verify this estimation correctly.

The study shows that the H/D ratio effect on the average bottom temperature is that lower the H/D ratio, the less the temperatures and the shorter cooling time since the flow effect response is higher. The other parameter observed with the study for the average bottom temperature is inclination of bottom. The study express that the inclination has affected negatively both cooling profile and time. Because, the nonuniform flow characteristic which is getting out from the jet nozzle becomes more if the inclination of bottom surface is getting increased.

The final monitor is putting blockage on the flow line. It is found that the blockage has significant effect to reduce average bottom temperature while the cooling time is increased. The reason of it is the first cooling effect of the flow on the bottom is getting lower whereas the heat transfer distribution is getting more uniform.

In conclusion, if the aim is reduce the average temperature of the surface, plater or something else, the jet nozzle should be closer to the surface with no inclination which is desired to cool and the air needs higher velocity. In addition to that, using blockage is evaluable option if the design allows to place it.

REFERENCES

[1] Caliskan, S., Baskaya, S., Calisir, T. (2014). Experimental and numerical investigation of geometry effects on multiple impinging air jets. *International Journal of Heat and Mass Transfer*, 75, 685-703.

[2] Dirita, C., De Bonis, M. V., Ruacco, G. (2006). Analysis of food cooling by jet impingement, including inherent conduction, *Journal of Food Engineering*, 81, 12-20.

[3] Gölcü, M., Yazıcı, H., Akçay M., Köseoğlu M. F., Sekmen, Y. (2012). Oto Camların Temperlenmesinde Çarpan Hava Jetleri ile Soğutmanın Deneysel İncelenmesi. *Makina Mühendisliği Bölümü*, Ankara, Turkey, 775-783.

[4] Jensen, M., Walther J. (2013). Numerical analysis of jet impingement heat transfer at high jet Reynolds number and large temperature difference, *Heat Transfer Engineering*, 34, 801-809.

[5] Jha, M., Ranikumar S., Sarkar I., Chakraborty S. (2016). Jet impingement cooling of a hot moving steel plate: An experimental study, *Experimental Heat Transfer*, 29, 615-531.

[6] Kalifa, R., Habli, S., Said, N. (2016). Parametric analysis of a round jet impingement on a heated plate. *International Journal of Heat and Fluid Flow*, 57, 11-23.

[7] Keshavarz, B., Green, S., Davy, M., and Eadie, D. (2011). Newtonian liquid jet impaction on a high speed moving surface. *International Journal of Heat and Fluid Flow*, 27, 1217-1225.

[8] Liu, Z., Feng, Z., (2011). Numerical simulation on the effect of jet nozzle position on impingement cooling of gas turbine blade leading edge. *Internal Journal of Heat and Mass Transfer*, 35, 4949-4959.

[9] Matthew, J., Dede, E., Garimella S. (2014). Local single and two phase heat transfer from an impinging cross-shaped jet, *International Journal of Heat and Mass Transfer*, 79, 432-436.

[10] Monnoyer, F., Lochegnies, D. (2008). Heat transfer and flow characteristics of the cooling system of an industrial glass tempering unit. *Applied Thermal Engineering, 28, 2167-2177.*

[11] Pingping, Y., Zhu, K., Shi, Q., Yuan, N., Ding, J. (2017). Transient heat transfer characteristics of small jet impingement on high temperature flat plate. *Internal Journal of Heat and Mass Transfer*, 8, 981-991.

[12] San, J., Lai M. (2001). Optimum jet-to-jet spacing of heat transfer for staggered arrays of impinging air jets, *International Journal of Heat and Mass Transfer*, 44, 3997-4007.

[13] Shukla, A., Dewan, A. (2017). Convective heat transfer enhancement using slot jet impingement on a detached rib surface. *Journal of Applied Fluid Mechanics*, 6, 1615-1627.

[14] Singh, D., Kohli, S. (2013). Numerical Simulation of the jet impingement cooling of a circular cylinder. *Numerical Heat Transfer*, 64, 153-185.

[15] Su, Z., Zheng, W., Zhang, Z. (2015). Study on diesel cylinder head cooling using nanofluid coolant with jet impingement, *Thermal Science*, 6, 2025-2037.

[16] Türkbaş, S., Ataer, Ercan. (2006). Camın temperlenmesinde ısıtma ve soğutma süreçlerinin karışık sınır şartlarında sayısal modellenmesi. *Makina Mühendisliği Bölümü*, Ankara, Turkey, 64, 727-738.

[17] Zhou, T., Xu, D., Chen, J., Cao C., Ye, T. (2016). Numerical analysis of turbulent round jet impingement heat transfer at high temperature difference. *Applied Thermal Engineering*, 100, 55-61.

[18] Yu, P., Zhu, K., Shi, Q., Yuan, N., Ding, J. (2017). Transient heat transfer characteristics of small jet impingement on high temperature flat plate, International Journal of Heat and Mass Transfer, 114, 981-991.

[19] Url-1 < *http://www.bakker.org/dartmouth06/engs150/07-mesh.pdf*>, data retrieved 15.04.2018.

[20] Url-2 < *http://www.cfd-online.com/Turbulence_modeling*>, data retrieved 20.04.2018.

APPENDICES

APPENDIX A: Figures

APPENDIX A

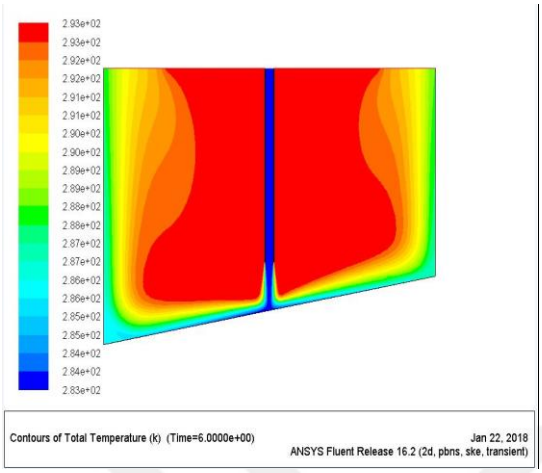

(a)

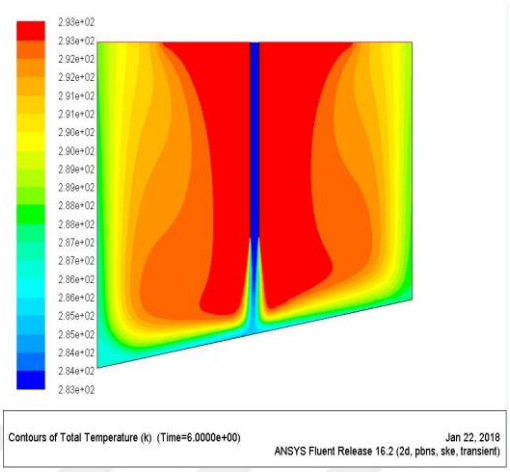

(b)

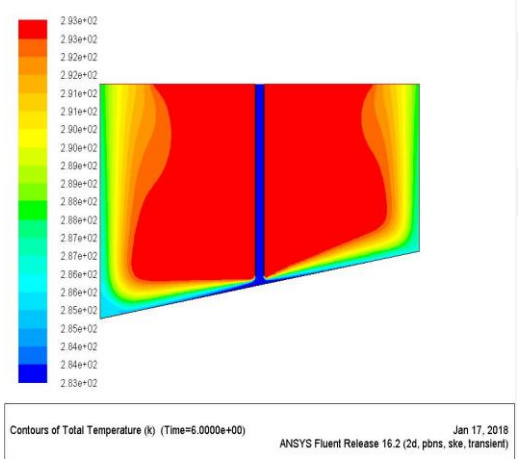

(c)

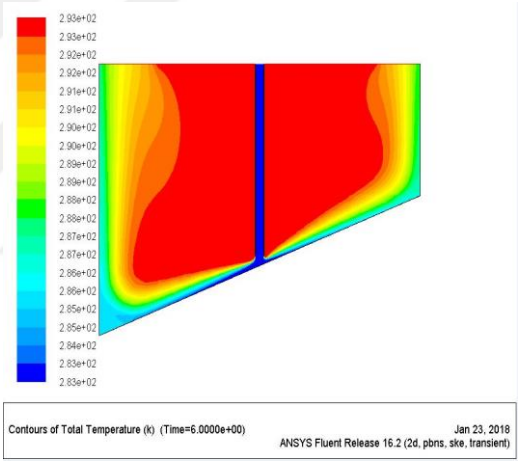

(d)

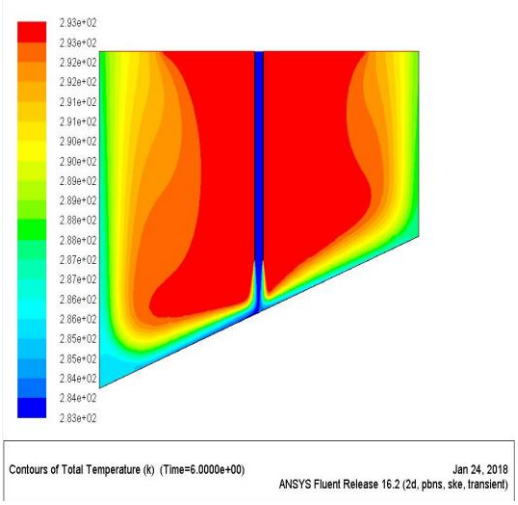

(e)

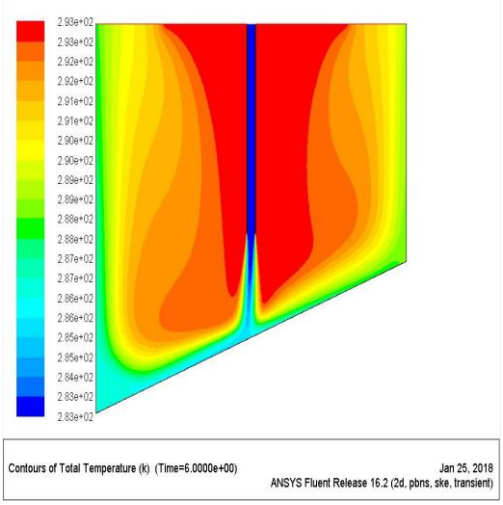

(f)

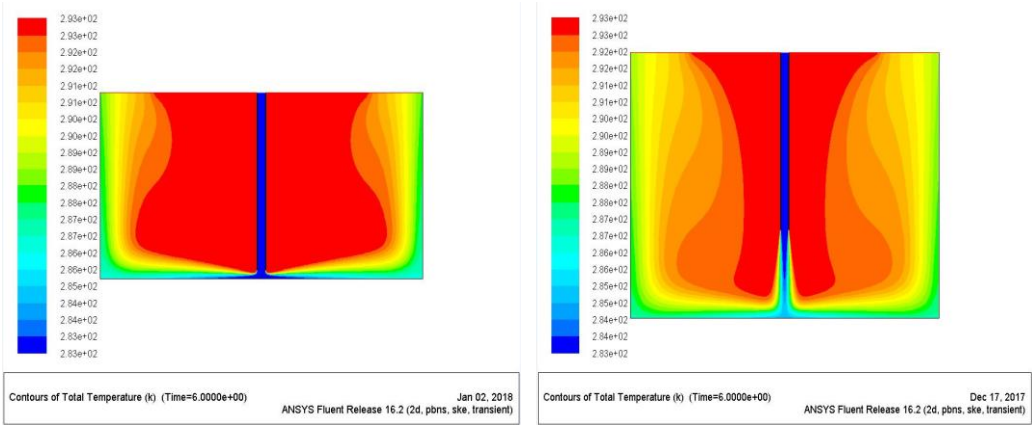

(g) (h)

Figure A.1 : Temperature distribution: (a)Re_6600_H/D_5_inclination_10. (b)Re_6600_H/D_10_inclination_10. (c)Re_6600_H/D_1_inclination_10. (d)Re_3300_H/D_1_inclination_20. (e)Re_3300_H/D_5_inclination_20. (f)Re_3300_H/D_1_inclination_20. (g)Re_6600_H/D_1_inclination_0. (h)Re_6600_H/D_10_inclination_0.

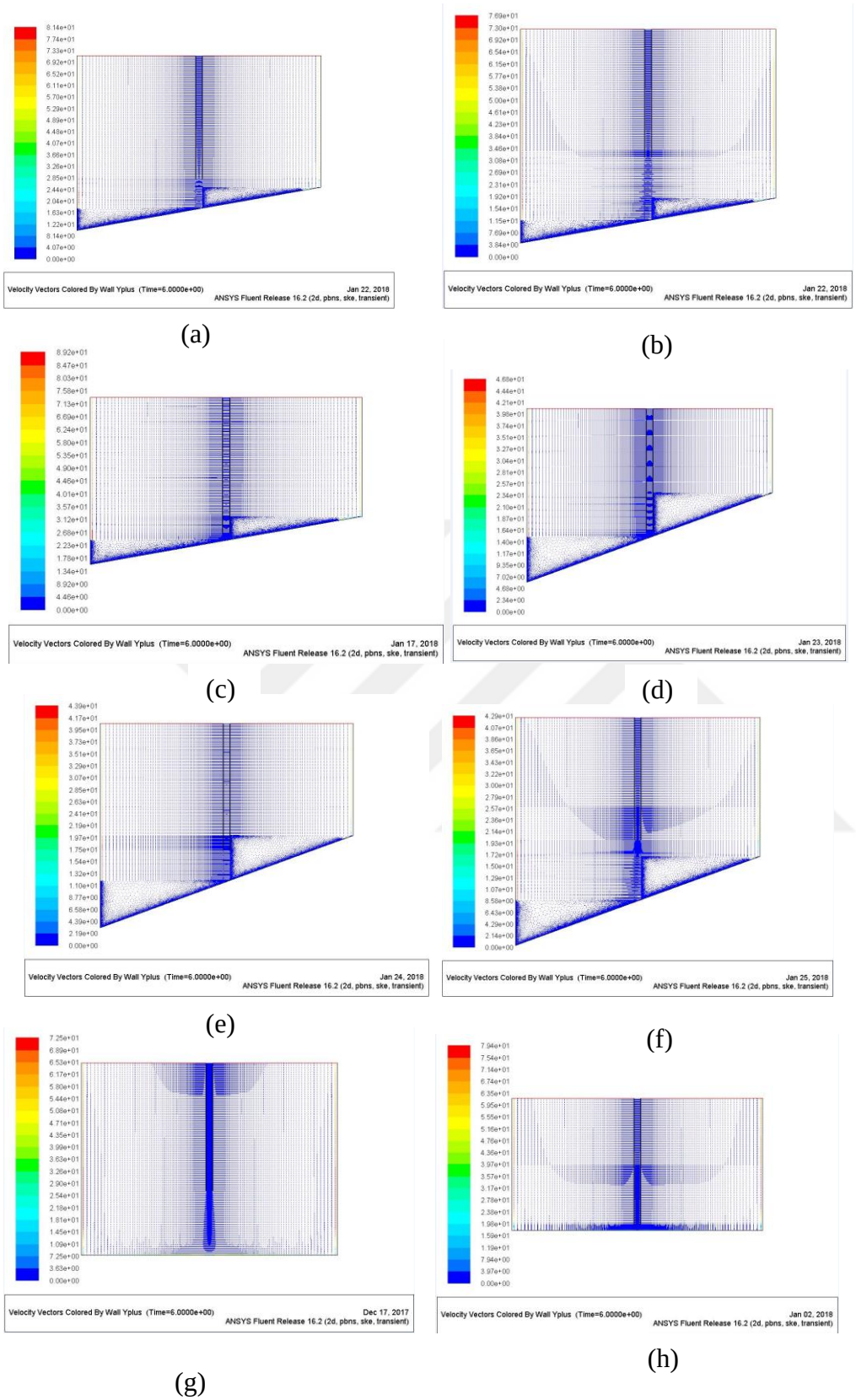

Figure A.2 : Y plus distribution: (a)Re_6600_H/D_5_inclination_10. (b)Re_6600_H/D_10_inclination_10. (c)Re_6600_H/D_1_inclination_10. (d)Re_3300_H/D_1_inclination_20. (e)Re_3300_H/D_5_inclination_20. (f)Re_3300_H/D_1_inclination_20. (g)Re_6600_H/D_1_inclination_0. (h)Re_6600_H/D_10_inclination_0.

CURRICULUM VITAE

Name Surname **:** Mehmet Fatih Bayar

Place and Date of Birth **:** 11/04/1990

E-Mail **:** mehmetfatihbayar@gmail.com

EDUCATION

- **B.Sc.** **:** Istanbul Technical University - Mechanical Eng.

PROFESSIONAL EXPERIENCE AND REWARDS:

- Ford OTOSAN R&D Center / P&E Engineer (2016 – present)

  Responsibilities include leading Ford Transit NA 1.5L which has 2 L panther diesel engine calibration project in terms of performance and efficiency and getting it in range of emissions.

- Ford OTOSAN R&D Center / FEAD Engineer (2015 - 2016)

  Responsibilities include leading Ford Transit and Ranger which have 2, 2.2 and 3.2 L diesel Puma and Panther engine front end accessory system responsible engineer to help launch support, voice of customer support.

- Ford OTOSAN R&D Center / OPD Engineer (2014 - 2015)

  Responsibilities include leading Ford Cargo vehicles which have 9L & 13L diesel Ecotorq engine for making attributes signoff plans, launch support, voice of customer support.